University of Kentucky
UKnowledge

University of Kentucky Master's Theses | Graduate School

2010

CHARACTERIZATION OF POLY(METHYL METHACRYLATE BASED NANOCOMPOSITES ENHANCED WITH CARBON NANOTUBES

Andrew Jonathan Placido
University of Kentucky, placido@caer.uky.edu

Right click to open a feedback form in a new tab to let us know how this document benefits you.

Recommended Citation

Placido, Andrew Jonathan, "CHARACTERIZATION OF POLY(METHYL METHACRYLATE BASED NANOCOMPOSITES ENHANCED WITH CARBON NANOTUBES" (2010). *University of Kentucky Master's Theses*. 62.
https://uknowledge.uky.edu/gradschool_theses/62

This Thesis is brought to you for free and open access by the Graduate School at UKnowledge. It has been accepted for inclusion in University of Kentucky Master's Theses by an authorized administrator of UKnowledge. For more information, please contact UKnowledge@lsv.uky.edu.

ABSTRACT OF THESIS

CHARACTERIZATION OF POLY(METHYL METHACRYLATE)-BASED NANOCOMPOSITES ENHANCED WITH CARBON NANOTUBES

The viscoelastic relaxation dynamics of a series of poly(methyl methacrylate) [PMMA] based nanocomposites filled with carbon nanotubes have been studied using dynamic mechanical analysis and broadband dielectric spectroscopy. The networks were prepared using four methods: (i) melt mixing, (ii) solution processing, (iii) in-situ polymerization, and (iv) polymer grafting. Nanotube modifications included surface oxidation via acid exposure and surface functionalization for polymer grafting. The effect of variations in processing method and nanotube modification on glass transition temperature (T_g) and relaxation dynamics was investigated. The relaxation behavior of the nanocomposites was sensitive to processing method and nanotube functionalization. Nanotube loading (to 5 wt%) led to a progressive increase in rubbery modulus, with the increase more pronounced in the solution-processed samples owing to enhanced nanotube dispersion. In the case of the oxidized nanotubes, loading led to an increase in modulus, but also a systematic decrease in T_g of ~ 15°C with 3 wt% nanotubes. For in-situ polymerized (PMMA/MWNT-ox) nanocomposites, there was no readily discernable trend in T_g. Composites prepared via in-situ polymerization in the presence of methyl methacrylate functionalized tubes (*i.e.,* polymer grafting) displayed a positive shift in T_g of nearly 20°C at 1 wt% loading. Investigation of the dielectric relaxation of the PMMA/MWNT composites indicated a percolation threshold between 0.3 and 0.4 wt% MWNT.

KEYWORDS: poly(methyl methacrylate), carbon nanotubes, nanotube functionalization, polymer nanocomposites, dynamic mechanical analysis

Andrew Jonathan Placido

April 12, 2010

CHARACTERIZATION OF POLY(METHYL METHACRYLATE BASED NANOCOMPOSITES ENHANCED WITH CARBON NANOTUBES

By

Andrew Jonathan Placido

Douglass Kalika
(Dr. Douglass Kalika, Co-Director of Thesis)

Barbara Knutson
(Dr. Barbara Knutson, Director of Graduate Studies)

April 12, 2010

RULES FOR THE USE OF THESES

Unpublished theses submitted for the Master's degree and deposited in the University of Kentucky Library are as a rule open for inspection, but are to be used only with due regard to the rights of the authors. Bibliographical references may be noted, but quotations or summaries of parts may be published only with the permission of the author, and with the usual scholarly acknowledgements.

Extensive copying or publication of the thesis in whole or in part also requires the consent of the Dean of the Graduate School of the University of Kentucky.

A library that borrows this thesis for use by its patrons is expected to secure the signature of each user.

Name	Date

THESIS

ANDREW JONATHAN PLACIDO

The Graduate School

University of Kentucky

2010

CHARACTERIZATION OF POLY(METHYL METHACRYLATE BASED NANOCOMPOSITES ENHANCED WITH CARBON NANOTUBES

THESIS

A thesis submitted in partial fulfillment of the
requirements for the degree of
Master of Science in Chemical Engineering
at the University of Kentucky

By

Andrew Jonathan Placido

Lexington, Kentucky

Director: Dr. Douglass Kalika, Professor of Chemical Engineering

Lexington, Kentucky

2010

Copyright ©Andrew Jonathan Placido 2010

ACKNOWLEDGEMENTS

The following thesis benefited from the insights and direction of several people. First, I must acknowledge Dr. Douglass Kalika for his guidance, support and direction over the last three years. He has taught me much about polymers and research as well as in the classroom. I am deeply grateful to him and I feel very fortunate to have had the opportunity to have him as an advisor. I would also like to thank Dr. Rodney Andrews and Dr. Mark Meier for their guidance and insight. I am also grateful to Dr. Matt Weisenberger for his help with polymer nanocomposite synthesis.

In addition to the guidance and technical assistance above, I received equally important assistance from family and friends. My parents, Tony and Denise Placido, provided on-going love and support throughout the thesis process. And finally, I would like to thank my friends, who know who they are, for keeping me sane during this period and enhancing the time I spent at the University of Kentucky.

TABLE OF CONTENTS

List of Tables

List of Figures

Chapter 1

Introduction and Objectives

The recent discovery of carbon nanotubes has led to a great amount of research on improving the macroscopic properties of polymers by incorporating the nanotubes into the polymer matrix. Carbon nanotubes are stronger and lighter than steel, while also having dimensions smaller than current fillers for nanocomposites.[1-2] Carbon nanotubes show superior mechanical, thermal and electrical properties, and even at relatively low loadings, the inclusion of nanotubes has been shown to enhance the macroscopic properties of polymers. However, while carbon nanotube composites have shown great promise, the inherent tendency to agglomerate has limited their successful application as nanoscale filler.

Poly(methyl methacrylate) has a wide variety of uses and is employed in many applications where strength and durability are needed such as medicine (bone cement), dentistry (dentures), and also as a low cost replacement for glass (Plexiglas®). Since poly(methyl methacrylate) offers superior macroscopic properties and is readily processable, it is an excellent candidate for the formulation of polymer nanocomposites based on the inclusion of nanotubes.

Due to the fact that carbon nanotubes are difficult to disperse with conventional polymer processing methods, new approaches have been developed to increase dispersion and reproducibility.[3-6] Melt mixing, solution processing, in-situ polymerization and polymer grafting have all been used as techniques to adequately disperse nanotubes within a polymer matrix. Recently, surface modification of the nanotubes has been performed in order to aid dispersion. Unfortunately, the resulting nanocomposites have all performed well below theoretical predictions. Therefore, current research is aimed not only at developing methods to disperse nanotubes adequately, but also to understand the nature of the interface between the polymer and the nanotubes, and its influence on bulk performance.

The goal of this study is to gain fundamental insight as to the influence of carbon nanotube surface chemistry on polymer-filler interactions and the corresponding enhancement of mechanical, electrical and thermal properties of the composites.

Specifically, the objective is to investigate the dynamic relaxation characteristics of a series of nanotube-loaded PMMA composites using dynamic mechanical analysis and dielectric spectroscopy. Key material variables include processing method, nanotube surface chemistry and overall nanotube loading.

Relevant background information on polymer nanocomposites and polymer thin films, as well as a review of the relaxation characteristics of PMMA, is presented in Chapter 2. Experimental methods used in this study are described in Chapter 3. The results for various series of PMMA-based polymer nanocomposites are presented in Chapter 4: melt mixed PMMA/MWNT, solution processed PMMA/MWNT and PMMA/MWNT-ox, and in-situ polymerized PMMA/MWNT-ox and PMMA/MWNT-MMA. Characterization methods include dynamic mechanical analysis, dielectric spectroscopy, thermogravimetric analysis and differential scanning calorimetry. Conclusions for the study are presented at the end of Chapter 4.

Chapter 2

Introduction and Background

2.1 Introduction

In order to predict the ultimate properties of nanotube-loaded polymer composites it is necessary to understand the nature of the polymer-nanotube interaction, and the extent to which the presence of the nanotubes perturbs the properties of the polymer matrix. The addition of nanoscale filler into polymer composites has been shown to create impressive enhancements in the electrical, mechanical and thermal properties of the resulting matrix.[7] The focus of this study is to gain an understanding of the influence that carbon nanotube surface chemistry has on polymer-filler interactions and the corresponding enhancement of the macroscopic properties. Insight into the relations between preparation method, nanotube dispersion and interfacial interactions, and their effect on bulk performance, is vital for formulating nanocomposites with the most advantageous properties. Poly(methyl methacrylate) [PMMA] was selected as the matrix polymer for this study due to its amorphous character (thereby avoiding potential complications related to crystallization), and its suitability for a wide range of production and processing techniques.

This chapter provides a review of polymer nanocomposites with a focus on multi-wall carbon nanotube [MWNT] filler and its influence on bulk polymer properties. Included is an examination of the fundamentals of polymer nanocomposite morphology and polymer-nanotube interactions as related to compositional factors, preparation methods and nanotube modifications.

2.2 Fundamentals of Polymer Nanocomposites

2.2.1 Polymer Matrix

Polymers are comprised of repeating structural segments and are found in a wide variety of everyday products. PMMA is a glassy amorphous polymer, with a glass transition temperature of ~100^{o}C. Due to its diverse range of applications and potential end-use environments, PMMA has been the subject of numerous nanocomposite studies focusing on the improvement of strength and durability.[3, 5-6, 8]

PMMA belongs to a subset of polymers referred to as amorphous. This group of polymers does not crystallize during the cooling process because they have semi-flexible or rigid backbone structures. The most important thermal transition in an amorphous polymer is the glass-rubber transition (T_g). The T_g is the narrow temperature range over which the amorphous polymer changes from the hard glassy state to the soft rubbery state. It is usually possible to assign T_g to a specific temperature using mechanical storage modulus, tanδ or the loss modulus. Polymers in the glassy domain, where the temperature of the surroundings is less than T_g, tend to be stiff and potentially brittle while polymers in the rubbery domain, are softer and more flexible.

2.2.2 Fillers for Polymer Nanocomposites

For a substantial number of applications, polymers are improved with additives or fillers. Fillers are incorporated into the polymer matrix for many uses including enhancement of processing and physical properties, and to add color. The addition of these fillers allows a single polymer to be adapted for many diverse purposes based solely on the material added to the matrix. For example, PMMA, since it is used in many applications that demand high optical quality, requires a filler to increase strength and toughness without masking its optical properties. In one such study, $MgCl_2$ was used as the filler creating a PMMA composite that would be suitable for use as an optical sensor[9].

With recent advances in nanotechnology, polymer nanocomposites have moved to the forefront of polymer research by using nanoscale fillers that produce superior physical properties but maintain the processing properties of the polymer[7, 10-11]. Nanoscale fillers offer significant advantages when compared to traditional fillers. Nanofillers are up to three orders of magnitude smaller than conventional fillers, and thus provide vast amounts of interfacial contact area. The large amount of interfacial volume that is created has properties that differ from the bulk polymer and provides the opportunity to tailor the overall polymer performance.

One of the most promising fillers under investigation for inclusion in polymer nanocomposites is carbon nanotubes [CNT]. CNT's are found in two forms: single-wall nanotubes (SWNT), and multi-wall nanotubes (MWNT). The latter are 10-40 nm

diameter, 10-100 μm long tubes similar in arrangement to graphite with cylinders axially aligned around a hollow core. **Figure 2.1** shows the structure of a carbon nanotube. MWNT's have been found to be almost 100 times stronger than steel at only 1/6 of the weight, and introduce large amounts of interfacial surface area. Carbon nanotubes also show superior mechanical, thermal, and electrical properties thus leading to high potential for their ability to improve composite properties.[2] Even at relatively low loadings, the inclusion of nanotubes has been shown to greatly enhance the macroscopic properties of polymers[6]. Unfortunately, due to the impurities and structural defects inherent in MWNT's, reproducible performance properties can be difficult to obtain and samples tend to vary from batch to batch.[1]

2.2.3 Polymer Nanocomposites

Polymer nanocomposites are defined as materials whose major component is a polymer and the minor component must have a single dimension below 100 nm. Polymer nanocomposites have become an active field of study in recent years because there have been accounts of large property changes with very small additions of nanofiller (less than 5 wt%). As with traditional composites, the most important element of the system is the interface. The interface is defined as the region in the vicinity of the filler surface where polymer properties are altered in comparison with the bulk.[12] The goal of understanding the interface between the nanofiller and the polymer is crucial for being able to optimize the properties for a particular function.

Two fundamental aspects that control the performance of polymer nanocomposites are the local interfacial properties and the resulting macroscopic changes in the composite. To determine the extent and the nature of the interactions at the interface, many techniques have been used including miscibility maps, dynamic mechanical analysis [DMA] and broadband dielectric spectroscopy [BDS]. The miscibility maps have been shown to provide a prediction of the dispersion the filler will have within the polymer, while DMA and BDS have been shown to measure the effect of the filler on dynamic mechanical and dielectric relaxation, respectively. Using all of these analytical techniques allows for the determination of macroscopic properties based on the changes in nanoscale properties at the interface. Dispersion and physical confinement

play a key role in determining macroscopic properties. Many techniques have been developed in order to distribute fillers evenly and efficiently thus producing composites with optimal properties throughout. Each dispersion strategy has the potential to influence the characteristics of the polymer matrix in the vicinity of the filler and will likely alter the distribution of mechanical, electrical and thermal loads across the interface.

Recently, MWNT's have been used as fillers in polymer nanocomposites due to their potential to impart large changes in macroscopic properties at low loadings. Models have indicated that MWNT's, even at low loadings, have an average separation distance comparable to the radius of gyration for elastic polymers.[13] Carbon nanotubes exhibit strong dispersive forces that limit solubility and encourage agglomeration. Due to the significant bundling tendency of carbon nanotubes, early investigators struggled to find appropriate processing methods that had the ability to disperse the nanotubes adequately throughout the matrix. Inadequate dispersion is the most cited process limitation in nanocomposites that contain MWNT's.[14] Eventually, viable processing methods were developed that provided satisfactory nanotube dispersions in the polymer matrix based on melt processing, solution blending and in-situ polymerization. Another technique used to improve dispersion within the polymer matrix involved chemically modifying the surface of the nanotubes, *e.g.* by polymer grafting. Recently, there have been studies where nanotubes are wrapped with a polymer thus disrupting the van der Waals forces that cause them to agglomerate and allowing the tubes to easily disperse throughout the polymer matrix.[15-16] These advances in polymer/nanotube composite formulation have greatly enhanced the quality of samples that can be produced.

2.2.4 Thin Polymer Films as a Model for Polymer Nanocomposites

It is generally accepted that the geometry and aspect ratio of the filler, as well as the interfacial shear stress of the composite, are the significant properties of traditional composites.[7] Fillers with high aspect ratios have more surface area with which to interact with the polymer and consequently influence the dynamics of the composite. Nanotubes, owing to their high aspect ratios, have shown a tremendous reinforcing capability.[10] It is also known that consistent dispersion and alignment of the filler is

crucial in establishing the properties of the composite. However, perhaps the most important factor in controlling macroscale properties in composites is the interface. Many studies have been performed on the interaction between the filler surface and the polymer chains. This is increasingly important in nanocomposites because the increased surface area of the filler increases the contact area with the polymer exponentially as compared to traditional composites.

Since the interface plays a crucial role in polymer nanocomposites, critical information can be obtained from thin polymer films. Polymer nanocomposites containing consistently spaced nanoparticles or nanotubes are in many respects analogous to thin polymer films in both their thermal and mechanical response behavior. Generally, nanoparticles are not distributed uniformly in the matrix and thus making a direct quantitative comparison between thin polymer films and nanocomposites is difficult. However, recently Bansal et al. have verified that polymer nanocomposites and thin polymer films are quantitatively equivalent in terms of their thermomechanical responses.[17]

There is a substantial amount that can be learned about polymer nanocomposites using thin polymer films as a model. In free-standing thin films, T_g decreases as a function of decreasing film thickness when specific interactions between the substrate and the polymer film are absent. On the other hand, the presence of strong, favorable interactions between substrate and polymer film leads to an observed increase in T_g.[18-20] Drawing a comparison to polymer nanocomposites, the glass transition, which is responsive to changes in the polymer matrix, increases in temperature if favorable interactions occur between the polymer and filler, presumably due to a reduction in polymer chain mobility in the vicinity of the interface. New studies also suggest that there is a correlation between the thickness of thin films and the interfacial spacing inherent to the polymer nanocomposite. From thin films, it is known that a surface can affect the polymer chains that are more than a radius of gyration away and that chemical interaction at the surface is the main parameter affecting T_g.[10] Using this fact to draw an analogy between thin films and polymer nanocomposites, T_g can be used as a measure of the polymer-filler interaction for polymer nanocomposites.

2.3 Preparation Methods for MWNT Nanocomposites

Preparation methods for exploiting the extraordinary physical properties of MWNT's in polymer nanocomposites have commonly focused on improving nanotube dispersion, because consistent distribution throughout the matrix has been shown to be an essential factor for the optimization of composite performance. The dispersion of native (*i.e.,* unmodified) nanotubes is particularly challenging, given their intrinsic thermodynamic tendency to cluster or agglomerate.[1] Nonetheless, the methods of melt mixing, solution blending, in-situ polymerization and grafting have all shown promise for adequately dispersing MWNT's within the polymer matrix.

2.3.1 Melt Mixing

Melt mixing is a common method employed to disperse nanotubes easily and uniformly throughout the polymer matrix. It uses high temperatures and high shear forces produced by counter rotating rotors to facilitate the dispersion. Melt mixing is an ideal method to produce MWNT composites because it is compatible with modern industrial processes and it is very effective in dispersing the nanotubes. However, melt mixing is a violent process due to the high shear forces produced. Nanotubes have been found to become broken, while the polymer structure may suffer damage because of the intense forces generated in melt mixing.

There have been many reports of well-dispersed samples produced by this process.[6, 8, 21-22] There have also been many variations of this process in order to lower viscosity of the polymer melt and improve compatibility of the MWNT's. One method employed by Haggenmueler et al. used both solvent casting and melt blending in a two step process.[21] Another variation of the melt mixing method was developed by Jin et al. that introduces nanotubes coated with polymer into the melt to increase compatibility.[4]

2.3.2 Solution Blending

Solution blending involves dispersion of nanotubes with high powered wand sonication in a low viscosity mixture. The low viscosity mixture is comprised of polymer

and nanotubes dissolved in a suitable solvent. After the nanotubes are sufficiently dispersed in the mixture the solvent is removed via evaporation or coagulation. Several studies have been performed to determine the appropriate solvent for various polymer/MWNT combinations. Liu et al. determined that the polar component of the solubility parameter was the most important parameter for predicting dispersion of nanotubes in the chosen solvent.[23] However, the ability of the solvent to dissolve the polymer is also an important factor to consider. Since some polymers are insoluble in common solvents, this method is only effective with certain polymer/CNT systems. Also, the final samples can retain residual solvent which lowers T_{g}.[4] Another drawback to solution blending is that high powered wand sonication has been known to damage the polymer chains and has even been found to shorten the nanotubes.[6, 14] However, the main reason this method is attractive is the excellent dispersion obtained due to the low viscosity of the mixture.

Solution blending has become the preferred method for producing PMMA/MWNT nanocomposites because it works well with small sample sizes and the dispersion is consistent and reproducible.[1] This method has also shown promising results in terms of producing PMMA/MWNT composites that have better electrical conductivity and thermal stability than pure PMMA.[5, 24-25] Good nanotube dispersions are common with this method, especially using the coagulation technique to "trap" the nanotubes within the precipitating polymer chains. Du et al. have tested the coagulation approach with PMMA and single-wall nanotubes, and subsequent analysis has proven the dispersion to be very good.[24]

2.3.3 In-situ Polymerization

In-situ polymerization begins by dispersing nanotubes into monomer and then polymerizing the dispersion. This method provides many of the benefits of solution blending such as good dispersion due to low viscosity and doesn't require the use of solvent to dissolve the polymer. However, in some cases the viscosity of the monomer may be too high and it is necessary to use solvent in order to aid dispersion. Unfortunately, the addition of solvent can interfere with the polymerization and reduces the length of the resulting polymer chains. In-situ polymerization is usually preferred to

solution blending because the nanotubes can potentially participate in the polymerization process.[26-30] Jia et al. reported that nanotubes can be initiated by AIBN to open their π-bonds, thus implying that they can participate in the polymerization and therefore form covalent bonds between the nanotubes and the PMMA matrix.[26] Composites made via this method have shown an increase in mechanical properties at modest levels of nanotube loadings, but at higher levels the composites become brittle.[26, 28] A major drawback to in-situ polymerization is the number of parameters that must be controlled in order to obtain consistent and reproducible composites. These parameters include polymerization temperature and time, initiator concentration, solvent content and the amount of agitation provided to disperse the nanotubes.

2.3.4 Polymer Grafting

Even though native nanotubes can potentially participate in the in-situ polymerization process, there is not always sufficient polymer-filler interaction to ensure adequate dispersion and corresponding composite enhancement. In order to create more interaction during polymerization, the nanotubes can be specifically functionalized to participate in the in-situ chain polymerization. Covalent functionalization of the nanotube surface followed by in-situ polymerization is referred to as polymer grafting. This method is used in order to incorporate the nanotube directly into the polymerization process. The functional groups on the nanotube surface are involved during polymerization therefore capturing the nanotube in place and guaranteeing covalent bonding between the polymer chains and the nanotubes. The resulting composites have shown an improvement in thermal and mechanical properties[31]. This method has proven to be highly successful in producing composites with increased dispersion and enhanced mechanical performance.[31-35]

2.4 Mechanical and Electrical Properties of MWNT Nanocomposites

Dynamic mechanical analysis and broadband dielectric spectroscopy have been used to examine the bulk performance properties and polymer chain relaxation behavior of a number of composites based on nanoscale fillers. MWNT nanocomposites exhibit improvements in stiffness and conductivity, and display promising performance

characteristics for a range of polymer product applications. The influence of MWNT's on the mechanical and electrical response characteristics of polymer nanocomposites as a function of loading and sample preparation are discussed below.

2.4.1 Mechanical Properties

2.4.1.1 Variation of Loading in MWNT Composites

Jin et al. have investigated the influence of MWNT loading on the mechanical behavior of PMMA/MWNT composites.[8] Networks were prepared using a melt processing method with MWNT loadings equal to 4, 9, 11, 17 and 26 wt%. The storage modulus of the composites was observed to increase as the loading increased. This was found to occur due to the stiffening effect of the nanotubes. It was also determined that as the temperature increased, the difference in storage modulus at each loading became more significant. A slight increase in T_g was observed with increasing nanotube content, showing that nanotubes hinder the segmental relaxation of the PMMA chains.

Andrews et al. also investigated the influence of nanotube loading on the mechanical behavior of MWNT/polymer composites.[36] In this study, they used polystyrene and polypropylene as the matrix polymers. The study showed that as nanotube concentration increased, both stiffness and strength were significantly improved. Andrews et al. took the investigation one step further and determined that functionalizing the surface of the nanotubes to improve interfacial adhesion could greatly increase tensile strength. When interfacial adhesion is weak, the nanotubes pull out of the matrix. By increasing the interfacial adhesion, an improvement in strength of the composite could be realized.

Even though it has been proven that nanotubes increase the strength and tensile modulus of polymer composites, the results remain well below theoretical predictions. Haggenmueller et al. reported that the addition of 5 wt% nanotubes increased the modulus of PE fiber.[37] However, theoretical models predict a modulus almost 10 times higher than the value reported in the study. It has been postulated that at high loadings, the improvement in mechanical properties that is observed could be limited by the high processing viscosity of the composites and the void defects that result.[38]

2.4.1.2 Variation of Preparation Method for MWNT Composites

Solution processed samples have been investigated in many studies. Both Cadek et al.[39] and Velasco-Santos et al.[40] obtained significant increases in stiffness and modulus for solution-based composites. The results suggest that good stress transfer can be attained at amorphous interfaces. Another report indicates that nanotubes produced by the chemical vapor deposition method are the optimum nanotubes for reinforcement of mechanical properties for solution processed samples due to the small diameter of tubes that are acquired via this method.[41]

Melt mixed samples have long been the easiest composites to make due to their compatibility with current industrial procedures. In many cases, however, only limited improvements in composite quality were reported. Meincke et al. for example, produced composites that more than doubled the modulus[42]. Unfortunately, the composites also displayed a reduction in ductility that caused a significant drop in impact strength of the samples. More recently, Zhang et al. were able to produce composites via melt mixing that had a three-fold increase in modulus with no reduction in ductility.[43-44] The remarkable results were credited to good dispersion, as well as interfacial adhesion that were confirmed by microscopy measurements.

In-situ polymerized samples can potentially lead to large increases in composite performance owing to high levels of local nanotube dispersion that are "locked-in" during the polymerization process. One study by Velasco-Santos et al. found that at a low loading of just 1 wt% MWNT, the modulus and strength increased by 1.5 times the values of the control.[31] Another study by Putz et al. obtained an increase in modulus that was close to the theoretical values that have been postulated for PMMA/MWNT composites.[29] These studies show the in-situ polymerization method has great promise for creation of polymer nanocomposites.

Nanotube functionalization can exploit the impressive properties of nanotubes in polymer nanocomposites due to the enhancement in interfacial interactions that are anticipated. Hwang et al. used a combination of PMMA and nanotubes with PMMA chains grafted to their surface to reinforce the composite.[45] The physical interaction they observed between the PMMA matrix and the nanotubes with the grafted chains

included a ten-fold increase in the modulus at a loading of 20 wt% nanotubes. This is significant because a good dispersion was obtained up to 20 wt% nanotubes, which is extraordinary. Similarly, they witnessed a progressive increase in modulus up to the final loading of 20 wt%, which was also unparalleled. This study focused on the physical interactions between PMMA and the nanotubes with grafted chains attached to their surface. It has also been postulated that grafting appropriate functional groups onto the nanotube surface that participate in the in-situ polymerization reaction could be used to establish covalent bonds between the functionalized tubes and the polymer chains, thus further enhancing the mechanical properties of the nanocomposite.[1-2, 7]

2.4.2 Electrical Properties

The molecular dynamics of MWNT nanocomposites have been investigated using broadband dielectric spectroscopy in a limited number of studies[46-48]. In all of these studies, a strong effect on the dielectric constant and loss is observed at very low loadings, ultimately leading to a percolation phenomenon that can occur at loadings as low as 0.3 wt% MWNT. This outcome is characterized by a sharp jump in the dielectric properties by many orders of magnitude and reflects the formation of a three dimensional conductive network of nanotubes in the polymer matrix.[1, 49-51] The percolation effect has also been determined to be dependent on the alignment of the nanotubes, with better alignment leading to percolation at lower loadings. Better alignment of the nanotubes lowers the percolation threshold of the composites by providing an easier pathway for the current to pass through the samples. Since the nanotubes cause dominant percolation effects at such low loadings, it is difficult to draw definitive conclusions as to the effect of MWNT's on polymer chain relaxation as detected via dielectric relaxation methods.

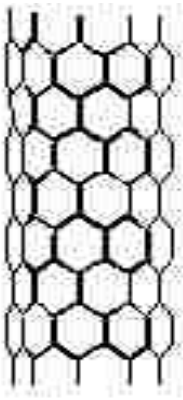

Figure 2.1: Representative drawing of a single-wall carbon nanotube (SWNT) showing the hexagonal lattice structure. In the case of a multi-wall nanotube (MWNT), there would be multiple nanotubes centered around a common hollow core. Nanotube figure used with the permission of UK-CAER.

Chapter 3

Experimental Methods

3.1 Materials

PMMA used in this work was Plexiglas® V826 resin and was provided by Altuglas International. Methyl methacrylate monomer [MMA] was purchased from Sigma-Aldrich (Milwaukee, WI). **Figure 3.1** shows the structure of the PMMA polymer. MWNT's were synthesized by the University of Kentucky Center for Applied Energy Research (Lexington, KY)[36, 52]. Also, in order to enhance polymer-nanotube interactions, encourage entanglements and promote covalent linkage with the polymer matrix, the as-prepared MWNT's were modified, as follows:

Modification 1: Oxidation of the as-received nanotubes began by refluxing with concentrated nitric acid overnight at 100°C. The tubes were than washed with deionized water until the pH was approximately 6. The resulting nanotubes had reactive carboxylic acid groups on their surface [MWNT-ox]. This method had a yield of 92.3%. **Figure 3.2** shows a representative schematic of the oxidation reaction of a MWNT.

Modification 2: Introduction of methyl methacrylate functional groups on the tube surface began by mixing liquid ammonia and lithium in order to create a solvated electron solution. The nanotubes were then added to the solution for 1 hr in order to add charge to the nanotubes. Next 3-bromo-1-propanol was added to the solution to attach hydroxyl-terminated reactive groups on the nanotube surface and left to react for 2 days. The nanotubes were then filtered out and dried overnight. Finally, the nanotubes were added to a mixture of methacryloyl chloride and toluene in order to functionalize the reactive groups and yield nanotubes with methyl methacrylate functional groups grafted on the surface. The nanotubes were left in the solution for 24 hours and were then filtered and dried overnight in the oven [MWNT-MMA].[53] **Figure 3.3** shows a representative schematic of the reactions a MWNT undergoes in order to add methyl methacrylate functionalization.

2,2′-azobisisobutyronitrile [AIBN] thermal initiator was obtained from Sigma-Aldrich, as was the N,N-dimethylformamide [DMF] solvent. All commercial materials were used as received.

3.2 Sample Preparation

The nanotube-filled polymer composite samples were prepared in four different ways: melt mixed, solution blended, in-situ polymerized and via a nanotube grafting technique. Each method has inherent benefits and drawbacks, as detailed below.

Melt Mixing:

The melt mixing technique disperses nanotubes into the polymer matrix using high temperature and high speed shear forces.[6, 8, 14, 21, 36] The melt mixing method is the best in terms of compatibility with industrial operations; however, the high shear forces needed to disperse the nanotubes also have the potential to break the tubes into shorter pieces.[1, 14] The damage to the tubes caused by the shear forces decreases the aspect ratio of the tubes but tends to increase their dispersability. Due to the high viscosity of the polymer in the melt state, the dispersion achieved using this technique is typically less than that obtained with the solution blending method.[1]

Commercial PMMA pellets were added to the Haake Rheomix (Vreden, Germany) and allowed to melt at 220^{o}C. MWNT's were then added to the molten PMMA and dispersed using high speed shear mixing with two counter-rotating stainless steel sigma-shaped rotors at 20 rpm. PMMA/MWNT nanocomposites produced via this method contained 0.1, 0.2, 0.3, 0.4, 0.5, 1.0, 3.0 and 5.0 wt% MWNT. A control sample of neat (i.e., unfilled) PMMA was also subject to the melt mixing procedure.

Solution Blending:

The second method employed to prepare the PMMA/MWNT nanocomposites was solution blending.[5, 25] This method is the most widely used method for dispersing nanotubes on the laboratory scale because it is effective and it can be used to fabricate small amounts of sample.[1] Solution processing begins by dispersing nanotubes in a solvent, followed by mixing with the chosen polymer that is dissolved in the same

solvent. The nanocomposite is then recovered via precipitation in water. This method is highly effective at dispersing nanotubes due to the low viscosity of the dissolved polymer solution. Recovering the nanocomposites via coagulation results in the nanotubes becoming trapped by the precipitating polymer chains and thus dispersion is maintained. However, because this method employs the use of high powered ultrasonication, there is also the potential for breaking or shortening the nanotubes, as was the case with the melt mixing method.[4, 24] An inherent drawback of the solution blending method is that it is unsuited for bulk/industrial processes due to the small amount of sample that can be prepared in this manner.

For the solution blending method, PMMA was dissolved in DMF resulting in a final concentration of 20 wt% PMMA. Meanwhile, an appropriate amount of as-received MWNT's was dissolved separately at a concentration of 0.25 wt% MWNT in DMF. The MWNT/DMF solution was then bath sonicated for 1 hour using the Fisher Sci. FS110H Ultrasonic Cleaner (Pittsburgh, PA) to disperse the nanotubes. Following the bath sonication, a suitable amount of the PMMA/DMF (20 wt% PMMA) solution was added to the MWNT/DMF solution so that a 3 wt% concentration of PMMA was present in the mixture. Adding a small amount of polymer before wand sonication is a good method to increase dispersion and reduce agglomeration of the nanotubes. The resulting mixture was high power wand sonicated for 5 minutes in increments of 30 seconds "on" and 10 seconds "off" using a Fisher Sci. Sonic Dismembrator 550 (Pittsburgh, PA). The remaining amount of the PMMA/DMF solution was added to the 3 wt% PMMA mixture and the combination was high-speed mixed using a Silverson L4RT Laboratory Mixer (East Longmeadow, MA). Finally, the PMMA/MWNT/DMF mixture was coagulated via drop-wise addition to a blender containing deionized H_2O. The product was recovered via vacuum filtration and then dried in a hood for two days followed by 24 hrs under vacuum at 120^{o}C. Samples made using the solution method contained 0.1, 0.2, 0.5, 1.0 and 3.0 wt% MWNT. Also, a control containing only PMMA was produced via the solution blending procedure. A second set of solution-prepared samples was produced using the oxidized nanotubes (MWNT-ox) instead of the as-received tubes, in the same concentrations.

In-situ polymerization:

A third method employed to disperse the nanotubes in the PMMA matrix was in-situ polymerization. In-situ polymerization was performed by free-radical thermal initiation within a suspension of MWNT's distributed in liquid methyl methacrylate monomer. **Figure 3.4** shows the polymerization of PMMA. The result of the polymerization is the formation of PMMA and also potentially covalent cross linking between the nanotubes and the surrounding polymer.[26-29, 31] An advantage of this method of dispersion is the ability to distribute the nanotubes in the pre-polymerization blend which has a low viscosity. Another advantage is being able to maintain the nanotube distribution as the reaction viscosity increases. Therefore, continuous sonication or physical stirring is not needed. According to Zhu et al., the reaction can also produce covalent cross-linking between the matrix and the nanotubes, leading to enhanced interfacial interaction.[38]

For the in-situ polymerization method, MMA monomer and DMF were mixed in a 1:1 ratio by weight. An appropriate amount of oxidized nanotubes (MWNT-ox) were added to the mixture and bath sonicated for 1 hour using the Fisher Sci. FS110H Ultrasonic Cleaner. The mixture was then high power wand sonicated at 20% power for 5 minutes total in increments of 30 seconds "on" and 10 seconds "off" using the Fisher Sci. Sonic Dismembrator 550. After sonication, the blend was heated to 80^{o}C and 0.20 wt% (based on weight of MMA) of the initiator (AIBN) was added in order to start the polymerization. After 24 hours of polymerization the sample was removed from heat and allowed to air dry overnight. The sample was then placed in a vacuum oven at 80^{o}C for 24 hours to remove any residuals. Samples made via this method contained 0.2, 0.5, 1.0, 2.0 and 3.0 wt% MWNT-ox. Also, an unfilled PMMA control was produced using this procedure.

Polymer grafting requires covalent functionalization of the surface of the nanotubes. The covalent functionalization can be achieved by direct addition of reagents to the nanotube wall or modification of the carboxylic acid groups that are known to be present on the oxidized nanotubes.[3, 34-35] "Grafting to" and "grafting from" are the two strategies that have been reported for the covalent attachment of polymer to the

nanotube. The "grafting to" approach results in polymers with reactive functional groups attached to the functional groups on the nanotube surface by chemical reaction. The advantage of this method is that commercial polymers can be used; however, the tethering of the polymer chains causes steric hindrance which leads to low grafting densities. The "grafting from" strategy involves the creation of initiation sites on the nanotube surface followed by polymerization of the polymer outward from the nanotube. Composites made via this technique can achieve very high grafting densities. Polymer grafting often involves the use of in-situ polymerization once the nanotube surface has been functionalized.

The "grafting from" technique was employed using an in-situ polymerization approach similar to that described above, but with the introduction of MMA-functionalized nanotubes [MWNT-MMA]. MMA monomer and DMF were mixed in a 1:1 by weight solution. An appropriate amount of MWNT-MMA's were added to the mixture and bath sonicated for 1 hour using the Fisher Sci. FS110H Ultrasonic Cleaner. The mixture was then high power wand sonicated at 20% power for 5 minutes total in increments of 30 seconds "on" and 10 seconds "off" with the Fisher Sci. Sonic Dismembrator 550. After sonication, the blend was heated to 80^{o}C and 0.20 wt% (based on weight of MMA) of the AIBN initiator was added in order to start the polymerization. After 24 hours of polymerization the sample was removed from heat and allowed to air dry overnight. The sample was then placed in a vacuum oven at 80^{o}C for 24 hours to remove residual solvent. Samples made via this method contained 0.2, 0.5, 1.0, 2.0 and 3.0 wt% MWNT-MMA.

3.3 Film Production

Samples films were prepared by compression molding using the Carver 25 ton bench top heated press (Wabash, IN). The as-prepared nanocomposite pellets were placed into a square mold of known thickness and then centered between the two heated platens of the press. The samples were pressed using 1500 psi into films of two thicknesses; approximately 0.3 mm for broadband dielectric spectroscopy [BDS] and 0.7 mm for dynamic mechanical analysis [DMA] studies.

3.4 Dynamic Mechanical Analysis [DMA]

3.4.1 DMA Theory

Dynamic Mechanical Analysis (DMA) is used to determine the mechanical response properties of polymers under oscillatory load; it is useful in determining the viscoelastic character of polymers, from the glassy to the rubbery state, over a specific range of temperature and oscillatory frequency. A polymer that behaves as a purely elastic solid follows Hooke's law, where the stress [σ] is proportional to the corresponding strain [ε] but is independent of the rate of strain. This behavior occurs at low temperatures and high rates of strain:

$$\sigma = E\varepsilon \qquad [3.1]$$

where E is the elastic modulus.

Similarly, polymers that behave as a viscous liquid can be modeled by Newton's law, where the stress is proportional to the rate of strain, but is independent of the strain. This occurs at high temperatures and low rates of strain:

$$\sigma = \eta \frac{de}{dt} \qquad [3.2]$$

In conventional DMA characterization, the polymer is subject to finite mechanical deformation at discrete frequencies where an oscillating strain is applied in a periodic manner and the resulting stress response is measured. DMA is helpful in determining the viscoelastic nature of polymers, from the glassy to the rubbery state, over a specific temperature range. Typically polymers act in a viscoelastic manner and the response of the stress lags the strain by an angle, δ. The relationship between stress and strain is given as:

$$\varepsilon = \varepsilon_0 \sin(\omega t) \qquad [3.3]$$

$$\sigma = \sigma_0 \sin(\omega t + \delta) \qquad [3.4]$$

where ω is the frequency of oscillation. Generally the response of the polymeric material is reported using the complex modulus. The complex modulus is simply the (time-dependent) stress divided by the strain, which can be represented as:

$$E^* = \frac{\sigma(t)}{\varepsilon(t)} = E' + iE'' \qquad [3.5]$$

where E′ is the storage modulus and E″ is the loss modulus. The storage modulus is a measure of the elastic response and is in-phase with the applied stain, while the loss modulus is a measure of the viscous response and is 90° out-of-phase with the applied strain (*i.e.,* in-phase with the rate of strain). The storage modulus and loss modulus are specified as:

$$E' = \frac{\sigma_0}{\varepsilon_0}\cos(\delta) \qquad [3.6(a)]$$

$$E'' = \frac{\sigma_0}{\varepsilon_0}\sin(\delta) \qquad [3.6(b)]$$

tanδ is called the loss factor and is the ratio of the viscous response to the elastic response. The loss factor establishes T_g, as well as the characteristic relaxation time of the transition, and is defined as:

$$\tan\delta = \frac{E''}{E'} \qquad [3.7]$$

A number of methods are available for analyzing DMA data, such as time-temperature superposition and the Kohlrausch-Williams-Watts stretched exponential function.[54-56] Since polymers are ideal for a vast array of commercial applications, the responses due to not only temperature but also time are needed. One drawback to DMA is the relatively small range of frequencies that are accessible in a typical experiment (10^{-1} to 10^2 Hz). In order to address this shortcoming, the time-temperature superposition method was developed based on the empirically-observed equivalence of time and temperature for rheologically-simple materials.[54] The Kohlrausch-Williams-Watts analysis method is a stretched form of the exponential decay function and can be used to

characterize the relaxation spectrum of the polymer. This model, when employed in conjunction with time-temperature superposition, is useful in establishing relaxation breadth on an objective basis.[55]

Figure 3.5 shows a schematic of a typical dynamic mechanical experiment with multiple frequencies. Results are reported via a semi-log plot of storage modulus and tanδ versus temperature. In this figure, the glass-rubber transition corresponds to the observed step change in modulus and corresponding peak in tanδ. T_g increases as the frequency increases due to the increased thermal energy required for the chains to respond to the mechanical deformation.

3.4.2 Experimental Design

Prior to measurement, all samples were dried in a vacuum oven to remove moisture and residual solvent. The samples were cut into rectangular bars approximately 17.5 mm long, 12 mm wide and 0.7 mm thick. DMA was performed using a TA Instruments Q800 DMA (New Castle, DE) configured in single cantilever bending geometry. **Figure 3.6** shows a typical experimental configuration in single cantilever geometry.[57] In this geometry the sample is clamped at both ends, with one end perturbed in a sinusoidal manner based on the chosen frequency. Storage modulus [E′] and tanδ were measured in temperature ramp mode (2^oC/min) from 35^oC to 180^oC at a frequency of 1 Hz. The experiments were all performed under nitrogen atmosphere.

3.5 Broadband Dielectric Spectroscopy [BDS]

3.5.1 BDS Theory

Broadband dielectric spectroscopy (BDS) is a technique that is employed to elucidate the localized, non-cooperative relaxations at sub-glass transition temperatures, and the more cooperative transitions near T_g of the composites. This method measures the dielectric response of the material when an alternating electric field is applied over a range of temperatures at specified frequencies. Commercial BDS instruments can reach frequencies as low as 10^{-3} and as high as 10^7 Hz. When the electric field is applied the composite becomes polarized, thus reorienting the atomic and molecular charges. Electronic polarization, orientation polarization and interfacial polarization are the

mechanisms by which the polarization is induced. Electronic polarization is an instantaneous displacement of electrons from their equilibrium position while orientation polarization is the realignment of the molecular dipoles of the polymer chain as a result of the alternating electric field. The final mechanism, interfacial polarization, is the movement and subsequent build-up of charge at the interface between phases.[58]

The focus of the BDS studies presented here will be on the orientation polarization mechanism because it provides insights as to polymer chain motions and the effect of the nanotube dispersion on polymer chain dynamics. Polymer chain motions encompass the large scale cooperative motions associated with the glass transition and also the non-cooperative relaxations of the sub-glass region such as vibration or rotation of a small portion of the polymer chain.[59-64]

3.5.2 Development of Phenomenological Equations

The parameters reported by the BDS instrument are dielectric constant (ε′) and dielectric loss (ε″). The dielectric constant corresponds to the in-phase portion of the polarization response, while the dielectric loss reflects the out-of-phase portion. Similar to DMA, tanδ, known as the dissipation factor in BDS, is the ratio of the dielectric loss to the dielectric constant. Phenomenological theories are used to relate the dielectric response from the instrument to the underlying dielectric properties.

Consider a capacitor in a parallel plate arrangement. The parallel plates have an electric charge applied across them and are separated by a fixed distance. Now consider that there is a polymeric material between the parallel plates that acts as a medium for the electric field, E. **Figure 3.7** depicts these scenarios. Polarization of the dielectric medium occurs when it is placed between the plates and the resulting capacitance is described by:

$$C = \frac{\sigma A}{Ed} \qquad [3.10]$$

where σ is the charge density, A is the area of the plates, and d is the distance between the plates. To simplify the capacitance relationship, the electric field can be represented as:

$$E = \frac{V}{d} \qquad [3.11]$$

where V is the potential difference across the plates. Also the charge density on the plates can be represented as:

$$\sigma = \frac{Q}{A} \qquad [3.12]$$

with Q representing the amount of charge on each of the plates. Combining the three previous relations yields the following definition for the capacitance across the plates:

$$C = \frac{Q}{V} \qquad [3.13]$$

As a result of having a dielectric material between the plates, the amount of stored energy in the capacitor increases which causes a subsequent loss in the strength of the electric field. However, if the dielectric medium is removed and instead a vacuum occupies the volume between the two plates, the capacitance across the plates would be reduced to C_0 based on the increase in the potential difference that would be required in order to maintain the charge at a constant level. Using this observation, the static dielectric constant can then be described by:

$$\varepsilon_s = \frac{C}{C_0} \qquad [3.14]$$

where C is the capacitance with a dielectric material and C_0 is the capacitance for vacuum. It is also possible to quantify the dielectric displacement, D, in terms of the static dielectric constant, or by using the polarization of the material, P.

$$D = \varepsilon_s E \qquad [3.15]$$

$$D = E + 4\pi P \qquad [3.16]$$

For BDS studies, a periodic electric field is applied to the material. The application of this time-dependent alternating field results in the dielectric displacement lagging the applied electric field. The periodic electric field is defined as:

$$E = E_O \cos(\omega t) \qquad [3.17]$$

Using the above definition, the analogous dielectric displacement can then be represented as:

$$D = D_O \cos(\omega t - \delta) = D_1 \cos \omega t - D_2 \sin \omega t \qquad [3.18]$$

where ω is the frequency of the electric field, t is the time and δ is the phase lag angle. The dielectric displacement represented above has two components: an in-phase portion and an out-of-phase portion. The in-phase component, D_1, is the real part while the out-of-phase component, D_2, is the imaginary part. Simplifying the periodic electric field and dielectric displacement equations results in two terms: dielectric constant (ε′) and dielectric loss (ε″). Using the dielectric constant and dielectric loss it is then possible to define the dissipation factor, tanδ. The dielectric constant and loss, along with the dissipation factor are defined below:

$$\varepsilon' \equiv \frac{D_1}{E_O} \qquad [3.19]$$

$$\varepsilon'' \equiv \frac{D_2}{E_O} \qquad [3.20]$$

$$\tan \delta = \frac{\varepsilon''}{\varepsilon'} \qquad [3.21]$$

PMMA and their nanocomposites display two distinct dielectric relaxation processes with increasing temperature. The lower temperature process, which is also known as the sub-glass transition, is designated as β. Similarly, the higher temperature process, corresponding to the glass-rubber transition, is labeled as α. The β transition is attributed to the methacrylate pendant groups undergoing local movements such as

rotation and vibration, while the α transition is due to full cooperative motions of the polymer chain. **Figure 3.8** shows a sample of the data for neat PMMA.

3.5.3 Experimental Design

In order to perform BDS studies, concentric silver electrodes with a radius of 33 mm were deposited on the sample films via thermal evaporation of silver pellets (Alfa-Aesar, Ward Hill, MA) using a VEECO 7700 Evaporator (Plainview, NY). The silver electrodes were needed to provide good electrical contact during the experimental measurements[65]. Once the films were coated, BDS sweeps were conducted using the Novocontrol Concept 40 Broadband Dielectric Spectrometer (Hundsangen, Germany). Samples were approximately 0.3 mm thick and inserted between two gold platens in a parallel plate arrangement[66]. **Figure 3.9** shows a sample configuration for a BDS experiment using the Novocontrol instrument. Dielectric constant and loss (ε′; ε″) were measured using a temperature ramp from -100^{o}C to 200^{o}C at 2^{o}C/min, with data recorded at 38 discrete frequencies between 1 Hz and 1 MHz. The WINFIT software package suite supplied with the BDS instrument was used to analyze the data.

3.6 Differential Scanning Calorimetry [DSC]

3.6.1 DSC Theory

Differential Scanning Calorimetry (DSC) is a widely-used method in polymer research that is employed to measure the heat effects of phase transitions of a sample material. Typically, DSC is used to identify phase transitions such as glass transition, melting, crystallization and decomposition. Commercial DSC instruments are comprised of two isolated cells. One cell (i.e., the reference cell) contains a reference sample or empty pan that is chosen so that the cell shows no transitions across the temperature range of the experiment. The other cell contains the experimental sample. The two cells are heated simultaneously so that both samples are maintained at the same temperature throughout the experiment. This can only be accomplished by providing more or less power to the sample of interest at certain times during the experiment. The differential heat flow delivered to the two samples to maintain the same temperature during the run is recorded in a DSC experiment. Temperature is usually ramped at a constant rate, so that

the important transitions can be distinguished such as the glass transition or crystalline melting of the material being studied. **Figure 3.10** shows a typical DSC curve and illustrates the form of the glass transition, crystallization and melting events.

3.6.2 Experimental Design

Circular samples approximately 3/8" in diameter were produced from thin films using a hammer and circular punch. Mass of the samples was kept at approximately 10 mg. The samples were sealed inside an aluminum pan using a crimping press while the reference cell contained an empty crimped aluminum pan. The atmosphere in both cells was kept inert using nitrogen. Experiments were performed using a TA Instruments Q100 DSC (New Castle, DE). Measurements were taken over a temperature range from 35-400^{o}C with a constant heating rate of 10^{o}C per minute. Some samples required a double heating cycle in order to remove residuals. For those samples, measurements were first taken from 35-200^{o}C heating at 10^{o}C/min. Then they were cooled back down to 35^{o}C at a rate of 5^{o}C/min. Finally, the samples were reheated to 200^{o}C at a rate of 10^{o}C/min.

3.7 Thermogravimetric Analysis [TGA]

3.7.1 TGA Theory

Thermogravimetric Analysis (TGA) is often used in polymer composite studies to determine the composition of a sample, as well as its degradation characteristics. The results of a TGA study are based on the change in mass of the sample as a function of temperature. In a standard experiment, a sample is placed in a pan of known weight and then both are heated at a constant rate within an insulated furnace. The measurement of the mass is very sensitive, with typical precision as low as 1 part per million. It is also possible to change the atmosphere during a TGA experiment. This is a beneficial technique because some compounds will not degrade in an inert atmosphere; however with the addition of oxygen at a specific temperature, the percentage of inert compounds within the sample can be more accurately calculated. TGA is readily used to determine moisture content, amount of residual solvent, degradation temperature, decomposition temperature and percentage of inorganic filler within the sample.

3.7.2 Experimental Design

Circular samples approximately 1/4” in diameter were punched out of thin films using a hammer and punch die. Mass of the samples was kept at approximately 30 mg so as to fit within the pan. The samples were placed in a platinum pan of known weight and loaded into the insulated furnace. The atmosphere was kept inert using nitrogen so that the nanotubes would not decompose. TGA was performed using a TA Instruments Q500 Thermogravimetric Analyzer (New Castle, DE). Measurements were taken over a temperature range from 35-800^{o}C with a constant heating rate of 20^{o}C per minute.

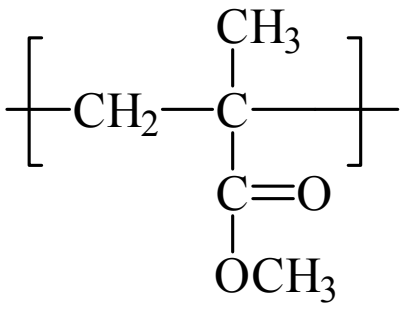

Figure 3.1: Repeating structure of PMMA

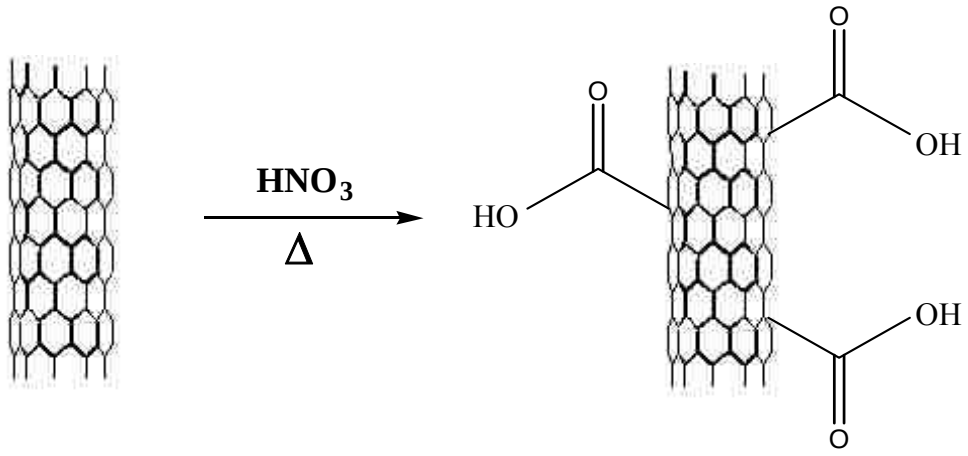

Figure 3.2: Schematic of modification 1: MWNT-ox. Schematic of carbon nanotubes used with permission of UK-CAER.

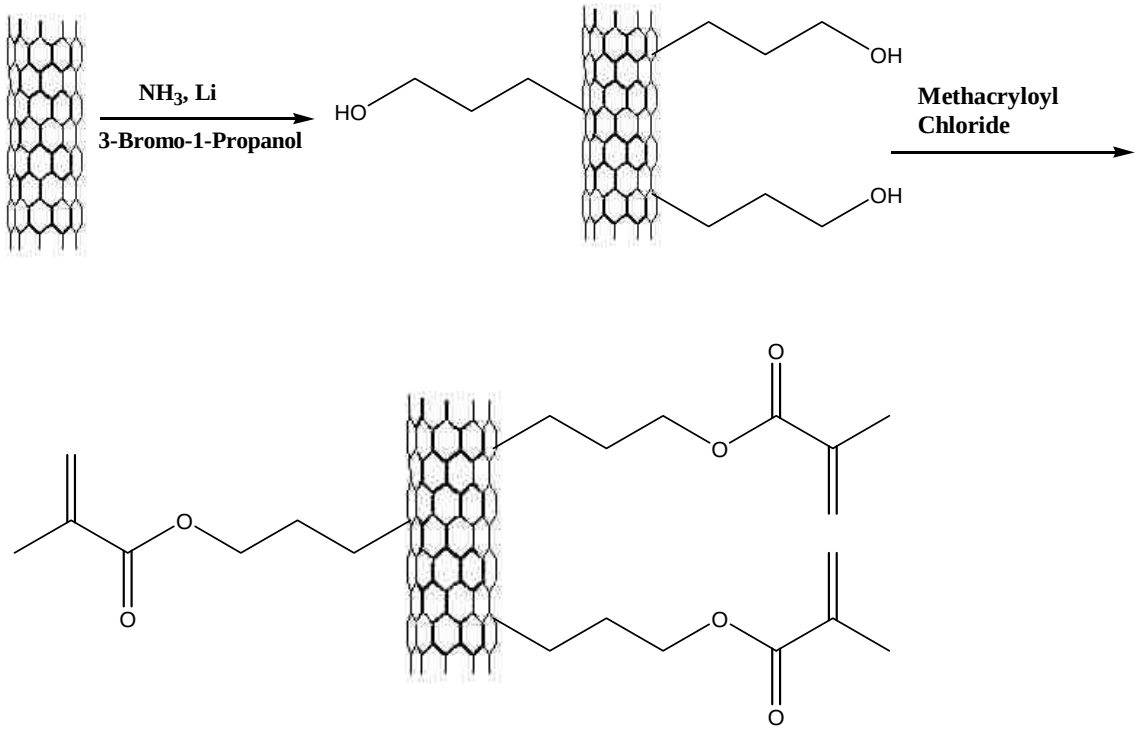

Figure 3.3: Schematic of modification 2: MWNT-MMA. Schematic of carbon nanotubes used with permission of UK-CAER.

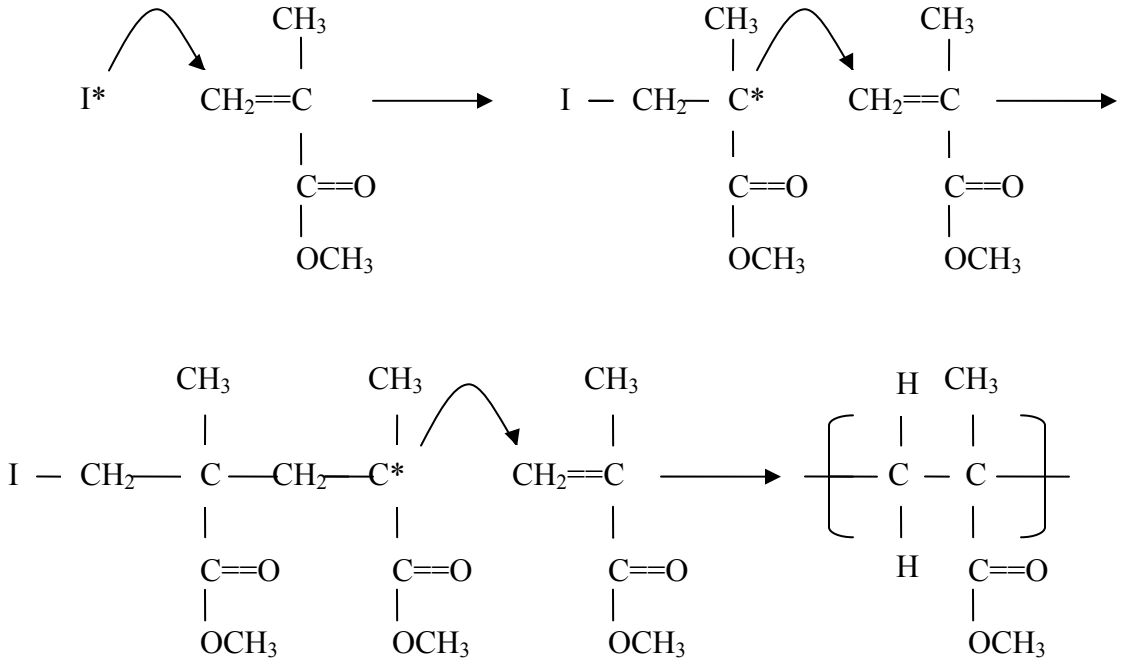

Figure 3.4: Representative schematic of in-situ polymerization reaction for PMMA.

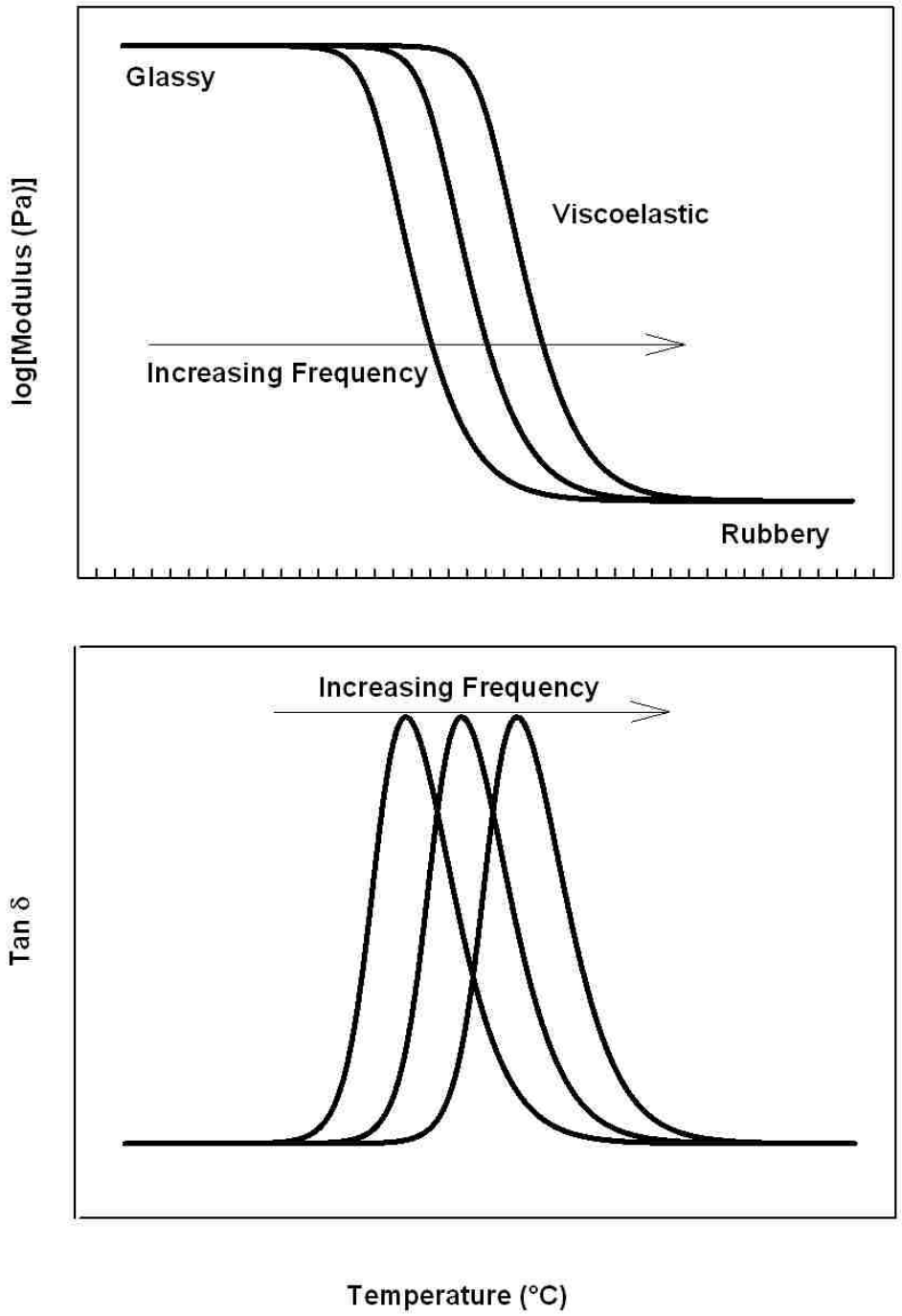

Figure 3.5: Typical DMA response of a characteristic polymeric material. Top plot: Storage Modulus [E′] versus temperature at discrete frequencies. Bottom plot: Tanδ versus temperature at discrete frequencies.

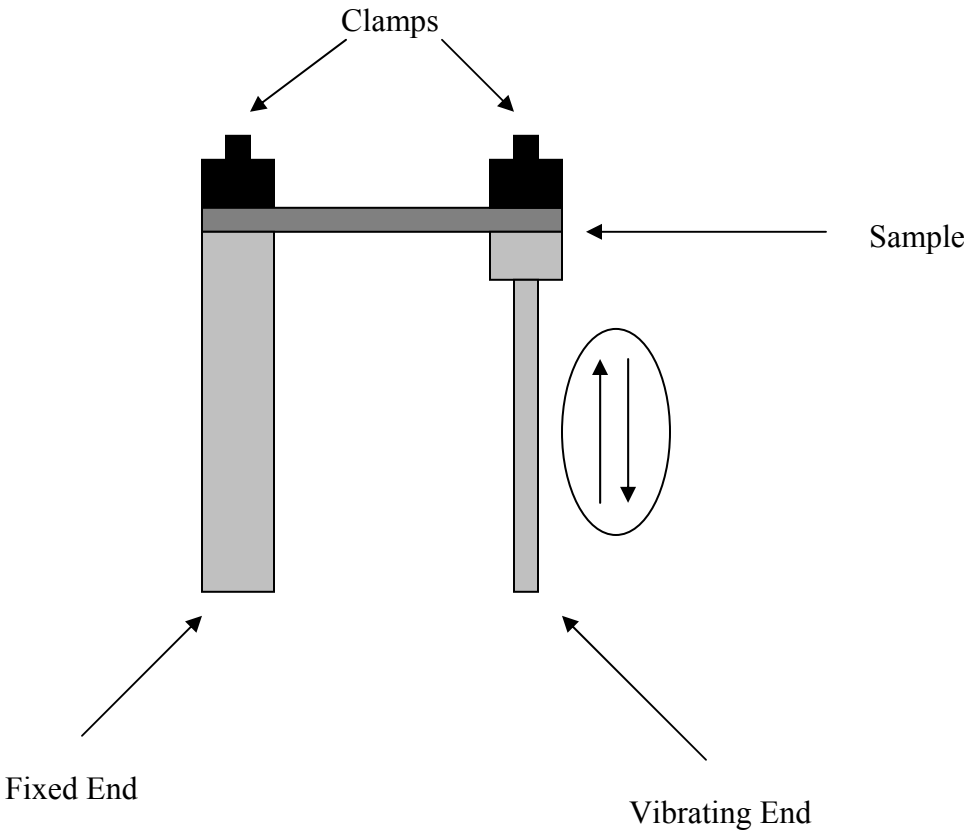

Figure 3.6: Typical DMA configuration; single-cantilever bending geometry.

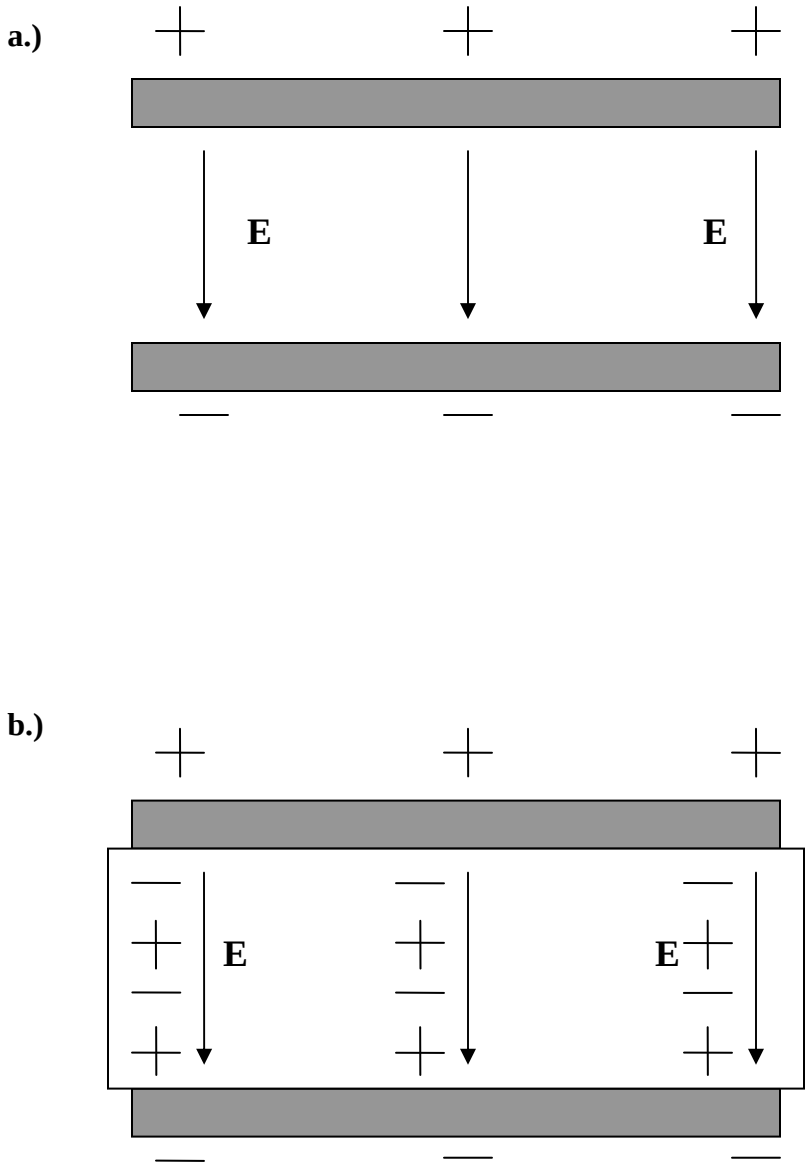

Figure 3.7: a.) Parallel plate capacitor in the absence of a polymeric medium. b.) Parallel plate capacitor with a polymeric medium creating polarization within the material

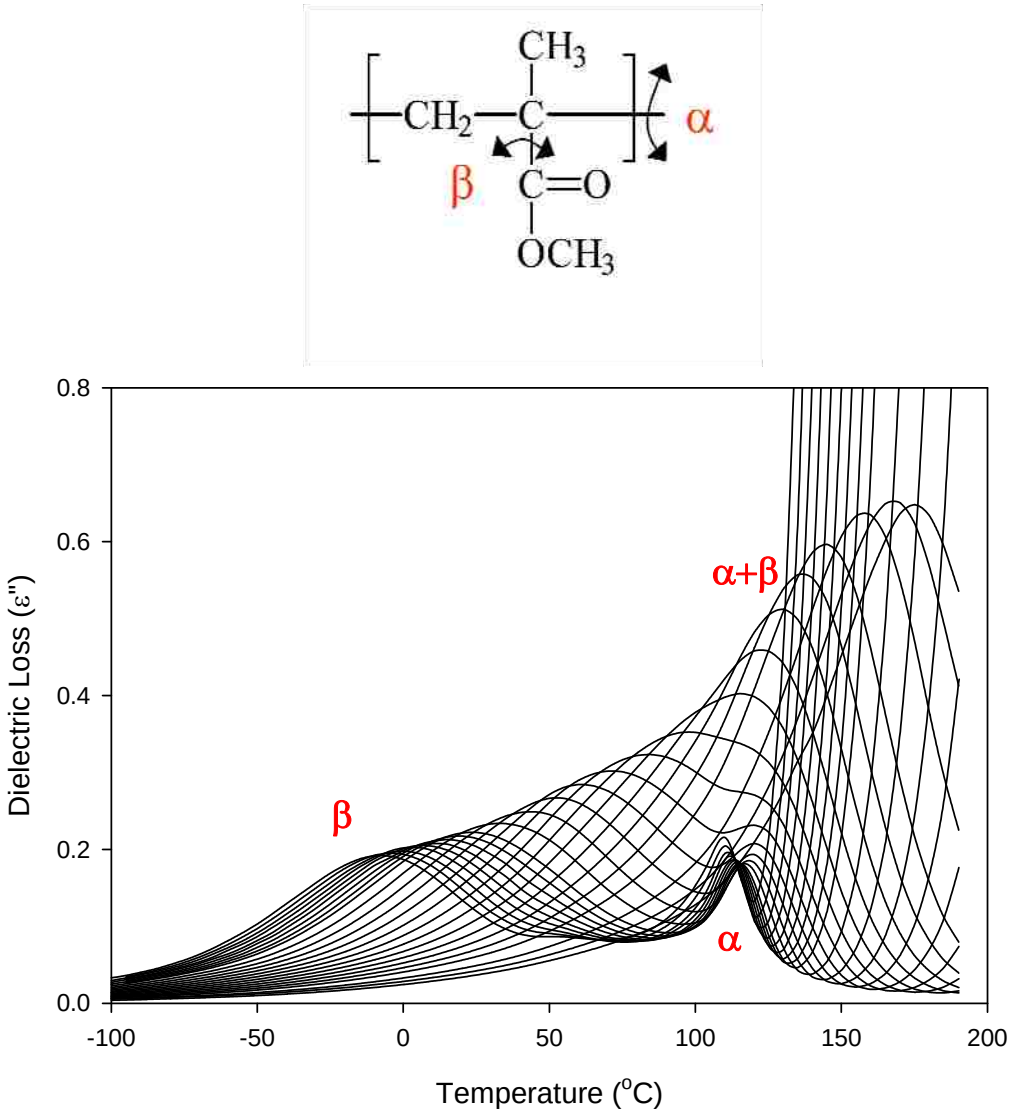

Figure 3.8: Representative broadband dielectric spectroscopy data showing the glass-rubber (α) and sub-glass (β) transitions; dielectric loss versus temperature at frequencies ranging from 1 Hz to 1 MHz.

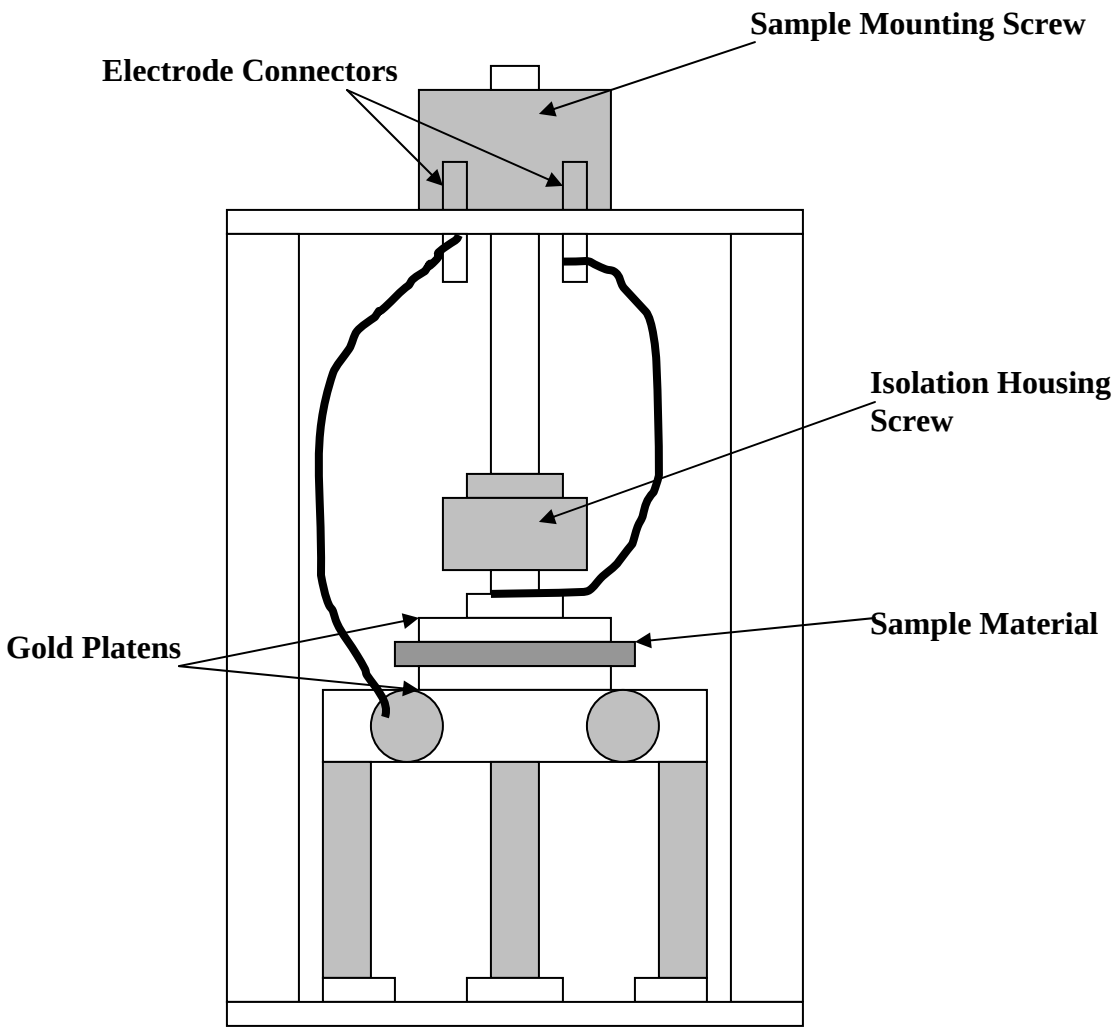

Figure 3.9: Novocontrol Concept 40 BDS experimental configuration

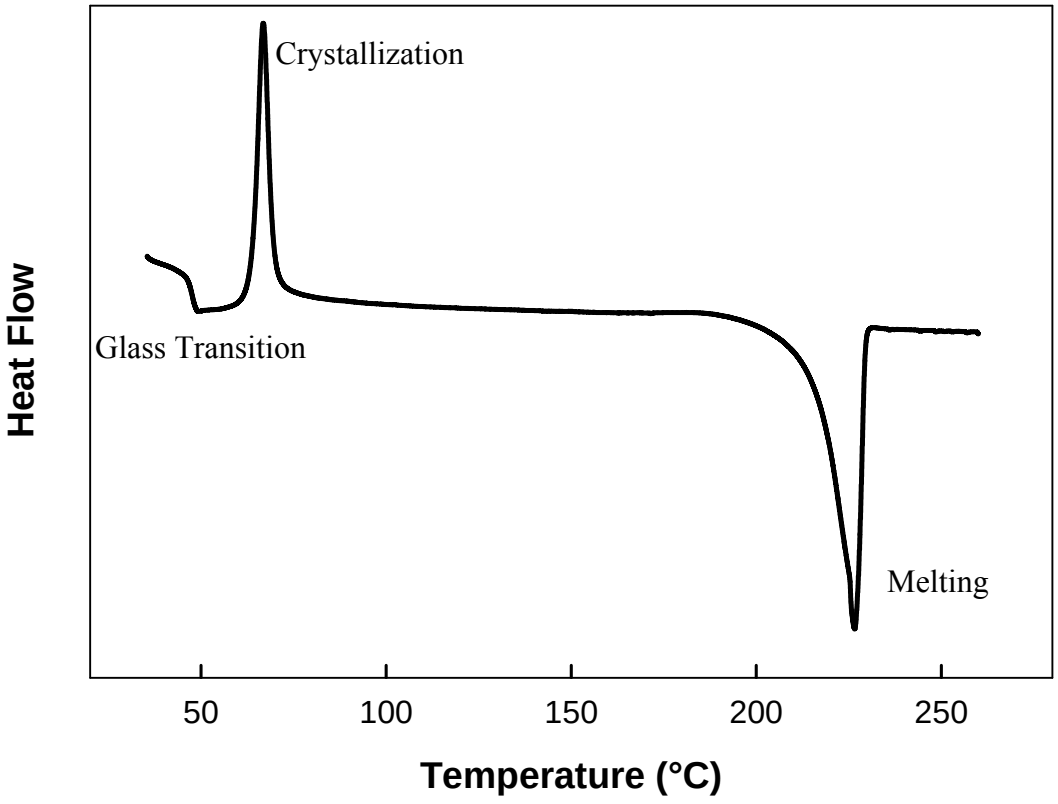

Figure 3.10: Typical DSC plot showing phase transitions for a semi-crystalline polymer.

Chapter 4

Viscoelastic Behavior of Poly(methyl methacrylate) Composites Enhanced with Multi-Wall Nanotubes

4.1 Introduction

The study of poly(methyl methacrylate) [PMMA] nanocomposites is of interest due to the numerous ways they can be employed in many different fields. PMMA has been included in applications such as bone cement in the medical field[6], dentures in the dental field[67], and as a low cost replacement for glass (Plexiglas®)[68-69]. Due to the diverse range of applications and the demanding environments that must be endured, PMMA has been the subject of numerous studies focusing on the improvement of strength and durability[3, 5-6, 8]. These studies have focused on adding a filler to the polymer matrix but have so far yielded limited success. However, the discovery of the extraordinary thermal, mechanical and electrical properties of carbon nanotubes (CNT's) in the early 1990's has brought renewed expectations for the enhancement of polymer properties. Even at relatively low loadings, the inclusion of nanotubes has been shown to greatly enhance the macroscopic properties of polymers.

Challenges for producing MWNT-polymer composites arise from the fact that MWNT's are hard to disperse in the polymer as they tend to agglomerate owing to strong dispersive forces that limit solubility. Several methods have been explored in order to produce a uniform dispersion of MWNT's within the polymer matrix. Melt blending[6, 8, 14, 21, 36], solution processing[5, 24], in-situ polymerization[26-29, 31] and polymer grafting[3, 34-35] have been the preferred methods to produce nanotube-filled nanocomposites.

Solution processing is the most common bench-scale method for producing nanocomposites because of effective dispersion, low agglomeration, and the small amount of sample needed. Melt blending is also an attractive technique because it works well with most industrial practices, produces bulk polymer nanocomposites, and can be used with polymers that are insoluble. This latter method relies on high temperature and high shear force to disperse the nanotubes within the polymer. Unfortunately, melt

blending does not disperse the nanotubes as efficiently as solution processing, but it is a much simpler process. However, both processes have their limitations. The high shear forces in the melt blending process can cause damage to the nanotubes and the polymer network. Also, during solution processing there is a possibility of excessive bath or wand sonication and this has the potential to break the nanotubes and degrade the polymer matrix.

In-situ polymerization and polymer grafting are two closely related methods. In-situ polymerization involves dispersing MWNT's in monomer and then polymerizing the mixture, thus capturing the nanotubes within the polymer matrix. Polymer grafting involves functionalizing the MWNT's so that the nanotubes participate in the polymerization. This method allows for the polymer to be covalently attached to the MWNT's. Both of these methods provide good dispersion due to the low viscosity of the starting mixture; however, they are also susceptible to the same problems as solution processing in that excessive wand sonication can damage the nanotubes and the functionalization on the nanotubes, and they involve the use of solvent which can affect both the polymerization and nanotube/polymer interaction.

In order to predict the ultimate properties of nanotube-polymer composites, it is necessary to understand the nature of the CNT-polymer interaction, and the extent to which the presence of the nanotubes perturbs the properties of the polymer matrix. This study is focused on investigating the influence of carbon nanotube surface chemistry on polymer-filler interactions and the corresponding enhancement of mechanical, electrical and thermal properties. Model composites were prepared using several methods that incorporate chemically-modified nanotubes in order to enhance the overall quality of the interface by dispersive forces, entanglements and covalent bonding within the matrix. The goal is to provide insight as to the relations between preparation method, nanotube dispersion and interfacial interactions, and their effect on bulk performance.

4.2 Materials and Methods

Poly(methyl methacrylate) [PMMA; MW = 132 kg/mol][70] resin was purchased from Altuglas International. The monomer used in this study, methyl methacrylate [MMA; nominal MW = 100.12 g/mol] was obtained from Sigma Aldrich (Milwaukee,

WI). 2,2′-azobisisobutyronitrile [AIBN] thermal initiator and N,N-dimethylformamide [DMF] solvent were also obtained from Sigma Aldrich. MWNT's were synthesized by the University of Kentucky Center for Applied Energy Research (Lexington, KY)[36, 52]. In order to enhance polymer-nanotube interactions, encourage entanglements and promote covalent linkage with the polymer matrix, the as-prepared MWNT's were modified using two different methods. In the first method, the nanotubes were oxidized by refluxing the tubes in a bath of concentrated nitric acid overnight. After washing with deionized water, the surface of the nanotubes contained reactive carboxylic acid groups[71]. In the second method, methyl methacrylate functional groups were grafted to the surface of the nanotubes. Details on the surface functionalization of the tubes is provided below.

Polymer samples with MWNT's as filler were prepared in four different ways: melt mixed, solution blended, in-situ polymerized and via a nanotube grafting technique. Melt mixed samples were prepared by adding commercial PMMA pellets to the Haake Rheomix (Vreden, Germany) and melting the polymer at 220^{o}C. MWNT's were added to the molten PMMA and dispersed using high speed shear mixing with two counter-rotating stainless steel sigma-shaped rotors at 20 rpm. The matrix was then allowed to cool resulting in a solid that was recovered for film production.

The second method employed to prepare the PMMA/MWNT nanocomposites was solution blending. For the solution blending method, PMMA was dissolved in DMF resulting in a final concentration of 20 wt% PMMA. Meanwhile, an appropriate amount of as-received MWNT's was dissolved separately at a concentration of 0.25 wt% MWNT in DMF. The MWNT/DMF solution was bath sonicated for 1 hour using the Fisher Sci. FS110H Ultrasonic Cleaner (Pittsburgh, PA) to disperse the nanotubes. Following the bath sonication, a suitable amount of the PMMA/DMF (20 wt% PMMA) solution was added to the MWNT/DMF solution so that a 3 wt% concentration of PMMA was present in the mixture. The resulting mixture was high power wand sonicated for 5 minutes in increments of 30 seconds "on" and 10 seconds "off" using a Fisher Sci. Sonic Dismembrator 550 (Pittsburgh, PA). The remaining amount of the PMMA/DMF solution was added to the 3 wt% PMMA mixture and the combination was high-speed mixed using a Silverson L4RT Laboratory Mixer (East Longmeadow, MA). Finally, the

PMMA/MWNT/DMF mixture was coagulated via drop-wise addition to a blender containing deionized water. The product was recovered using vacuum filtration and then dried in a hood for two days followed by 24 hrs under vacuum at 120^{o}C. Using this method, a fine powder was recovered for film production.

The third method employed to disperse the nanotubes in the PMMA matrix was in-situ polymerization. For the in-situ polymerization method, MMA monomer and DMF were mixed in a 1:1 ratio by weight. An appropriate amount of oxidized nanotubes (MWNT-ox) were added to the mixture and bath sonicated for 1 hour using the Fisher Sci. FS110H Ultrasonic Cleaner. The mixture was then high power wand sonicated at 20% power for 5 minutes total in increments of 30 seconds "on" and 10 seconds "off" using the Fisher Sci. Sonic Dismembrator 550. After sonication, the blend was heated to 80^{o}C and 0.20 wt% (based on weight of MMA) of the initiator (AIBN) was added in order to start the polymerization. After 24 hours of polymerization the sample was removed from heat and allowed to air dry overnight. The sample was placed in a vacuum oven at 80^{o}C for 24 hours to remove any residuals. A solid mass was recovered via this method for film production.

The last method employed was the polymer grafting technique**.** The "grafting from" technique was employed using an in-situ polymerization approach similar to that described above, but with the introduction of MMA-functionalized nanotubes [MWNT-MMA]. Introduction of methyl methacrylate functional groups on the tube surface was initiated by filling a 100L stirred reactor flask approximately half full with liquid ammonia and then adding 25g of lithium in order to create a solvated electron solution. Then, 10g of the nanotubes were added to the solution for the purpose of adding charge to the tubes. Next, 100g of 3-bromo-1-propanol was added to the solution to attach reactive groups to the nanotube surface and was left to react for 2 days with continuous stirring. The nanotubes were then filtered out and dried. Finally, the nanotubes were added to a mixture of 1L of methacryloyl chloride and 1L toluene in order to functionalize the reactive groups and yield nanotubes with methyl methacrylate functional groups grafted on the surface. The nanotubes were left in solution for 24 hours and were then filtered and dried overnight *in vacuo*.[53] **Figure 4.1** shows a schematic of the functional group that was attached to the surface of the nanotubes via this procedure.

The nanocomposites were prepared using in-situ polymerization according the method described above, but with functionalized nanotubes instead of oxidized tubes. Appropriate amounts of MWNT-MMA filler were added to the mixture of monomer and DMF. The blend was polymerized with AIBN and then allowed to air dry at the conclusion of the polymerization. Finally, the samples were placed in a vacuum oven to remove residual solvent and the recovered material was a solid mass.

Recovered samples from each of the methods were melt-pressed into uniform films for testing. Films were prepared by compression molding using the Carver 25-ton bench top heated press (Wabash, IN). The recovered nanocomposite pellets were placed into a square mold of known thickness and then centered between the two heated platens of the press. The samples were pressed using 1500 psi into films of two thicknesses; approximately 0.3 mm for broadband dielectric spectroscopy [BDS] and 0.7 mm for dynamic mechanical analysis [DMA], thermogravimetric analysis [TGA] and differential scanning calorimetry [DSC] studies.

Dynamic mechanical analysis was conducted using a TA Instruments Q800 DMA (New Castle, DE). The samples were cut into rectangular bars approximately 17.5 mm long, 12 mm wide and 0.7 mm thick. All measurements were performed in single cantilever geometry. Storage modulus [E′] and tanδ were measured in temperature ramp mode (2^{o}C/min) from 35^{o}C to 180^{o}C at a frequency of 1 Hz. The experiments were all performed under nitrogen atmosphere.

Thermogravimetric analysis was performed using a TA Instruments Q500 Thermogravimetric Analyzer (New Castle, DE). Circular samples approximately 1/4” in diameter were punched out of thin films using a hammer and punch die. Mass of the samples was kept at approximately 30 mg. The samples were placed in a platinum pan of known weight and loaded into the insulated furnace. Measurements were taken over a temperature range from 35-800^{o}C with a constant heating rate of 20^{o}C per minute. The atmosphere was kept inert using nitrogen for the duration of the experimental run.

Differential scanning calorimetry was performed using a TA Instruments Q100 DSC (New Castle, DE). Circular samples approximately 3/8” in diameter were produced from thin films using a hammer and circular punch. Mass of the samples was kept at approximately 10 mg. The samples were sealed inside an aluminum pan using a

crimping press while the reference cell contained an empty crimped aluminum pan. The atmosphere in both cells was kept inert using nitrogen. Measurements were taken over a temperature range from 35-400^{o}C with a constant heating rate of 10^{o}C per minute. Some samples required a double heating cycle in order to remove residuals. For those samples, measurements were first taken from 35-200^{o}C heating at 10^{o}C/min. Then, they were cooled back down to 35^{o}C at a rate of 5^{o}C/min. Finally they were reheated back to 200^{o}C at a rate of 10^{o}C/min.

Broadband dielectric spectroscopy sweeps were conducted using the Novocontrol Concept 40 Broadband Dielectric Spectrometer (Hundsangen, Germany). Concentric silver electrodes with a radius of 33 mm were deposited on the sample films via thermal evaporation of silver pellets (Alfa-Aesar, Ward Hill, MA) using a VEECO 7700 Evaporator (Plainview, NY). Once the films were coated, the samples (approximately 0.3 mm thick) were inserted between two gold platens in a parallel plate arrangement.[66] Dielectric constant and loss (ε'; ε'') were measured using a temperature ramp from -100^{o}C to 200^{o}C at 2^{o}C/min, with data recorded at 38 discrete frequencies between 1 Hz and 1 MHz.

4.3 Results and Discussion

4.3.1 Melt Processed Samples

Melt processing has been a popular method for the dispersion of nanotubes in recent years. High temperatures are used to melt the polymer and then shear forces from counter-rotating rotors are used to disperse the nanofiller. The melt processing method is often preferred owing to its suitability for bulk processing and compatibility with current industrial production operations. Unfortunately, the high viscosity of the polymer melt can limit dispersion of the filler. In addition, the high shear forces needed to distribute the tubes can decrease their aspect ratio while simultaneously damaging the polymer chains.

Thermogravimetric analysis was employed in order to examine the composition of each sample. **Figure 4.2** shows thermogravimetric results for the melt mixed set of samples ranging from the control up to 5 wt% MWNT. The unmodified nanotubes were used for these samples. Data were recorded from 35 to 800^{o}C. A major decomposition event occurs around 400^{o}C for all samples in the plot. This event is due to polymer chain

pyrolysis at high temperature. There is also a slight shift to higher temperatures of the decomposition event with increasing loading. After the decomposition event at 400^{o}C the entire organic content should be removed from the sample and only nanotubes and small amounts of residuals (e.g. catalyst) should remain. **Figure 4.2** also includes an expanded view of the TGA results (400 to 800^{o}C). Using the control experiment as a baseline, it is a simple calculation to determine the nanotube concentration of each sample: nanotube concentration was defined as any remaining material in a given experiment at 800^{o}C minus the baseline at 800^{o}C. **Table 4.1** shows the nominal (preparation) loading values and the measured values that were calculated using TGA results. The nominal values and the actual values are very close; for convenience, the preparation values will be used when referring to these samples.

Figure 4.3 shows dynamic mechanical results for the melt mixed PMMA/MWNT samples. Data were recorded at 1 Hz from 35 to 180^{o}C. A strong step change in the storage modulus (E') is evident beginning around 120^{o}C for all samples. This step change is an indication of the glass-rubber relaxation process which also appears as a peak in the tanδ curve. The glass-rubber transition peak temperature does not change significantly for any of the nanocomposite samples regardless of loading. Even though the glassy modulus remains nearly constant with nanotube loading, the rubbery modulus shows a progressive increase at higher loadings as the nanotubes stiffen the polymer matrix, consistent with the results of Schwarzl et al.[72] Thus, the step change from the glassy modulus to the rubbery modulus for the 3 wt% and 5 wt% loadings is much less than for the other samples. This effect can also be observed in the tanδ curves where the peak intensities for the 3 wt% and 5 wt% samples are much lower than the other samples. For example, the tanδ peak magnitude of the 5 wt% MWNT sample is reduced by one-half as compared to the unfilled control. While the tanδ peak intensity decreases at higher loadings, the glass transition temperature remains nearly constant at ~ 128^{o}C. This suggests that the nanotubes and polymer are not interacting in any discernable manner and that the stiffening of the composite is due solely to the reinforcing effect of the nanotubes. If either favorable or unfavorable interactions were occurring a significant change in T_g would be anticipated.

Broadband dielectric spectroscopy (BDS) was used to examine the sub-glass and the glass-rubber transitions of the nanotube-enhanced PMMA composites. PMMA and their nanocomposites display two distinct dielectric relaxation processes with increasing temperature. The lower temperature process, which is also known as the sub-glass transition, is designated as β. Similarly, the higher temperature process, corresponding to the glass-rubber transition, is labeled as α. The β transition is attributed to the methacrylate pendant groups undergoing local movements such as rotation and vibration, while the α transition is due to full cooperative motions of the polymer chain.

Figure 4.4 shows the dielectric relaxations of the melt-mixed samples at 30 Hz. The melt mixed data reveal an increase in the intensity of both the β and α transitions with increasing nanotube loading, but no apparent shift in relaxation temperature in the nanocomposites. The 30 Hz frequency was chosen because it shows the two distinct transitions (β and α) before they merge at higher testing frequencies. Low loadings were used in BDS measurement because at higher loadings, percolation of the highly-conductive nanotubes was encountered, leading to a short-circuit pathway that precludes traditional dielectric measurement at loadings above ~ 0.3 wt%. In a related study, Logakis et al. used polyamide filled with MWNT's and observed that only the sample with the lowest loading could be analyzed using BDS due to the percolation threshold. Any sample tested that was over the percolation threshold resulted in dielectric relaxations masked by conduction.[73]

4.3.2 Solution Processed Samples

4.3.2.1 PMMA/MWNT Composites

The second method employed to prepare the PMMA/MWNT nanocomposites was solution blending. This method is most commonly used on the laboratory scale, with small batches and good quality nanotube dispersion. Solution processing begins by dispersing nanotubes in a solvent, followed by mixing with PMMA that is also dissolved in the same solvent. The nanocomposite is then recovered via precipitation in water. This method is highly effective at dispersing nanotubes due to the low viscosity of the polymer solution; also, as the polymer chains precipitate out of the solution, the nanotubes become physically trapped and are held in place within the matrix. However, because this method

employs high powered ultrasonication, there is the potential for breaking or shortening the nanotubes, as was the case with the melt mixing method. An inherent drawback of the solution blending method is that it is unsuitable for bulk/industrial processes due to the small amount of sample that can be prepared in one batch.

Thermogravimetric analysis results for the solution processed PMMA/MWNT series are reported in **Table 4.2**. These samples were also prepared using the unmodified nanotubes. The table shows the nominal preparation values and the measured values that were determined using TGA; here again, the preparation values and the measured values are very close. Note that at higher loadings, the measured values are slightly lower than the preparation values, and also lower than the equivalent melt processed samples. This may be due to the fact that when the nanocomposite samples were precipitated out of solution using anti-solvent, some nanotubes may have been lost (i.e., not trapped in the coagulated sample), resulting in a lower overall loading. In melt processing, there is no point in the preparation for the nanotubes to escape, and therefore the measured loading values for melt processing were slightly higher than for the solution processed series.

Figure 4.5 shows dynamic mechanical results for the solution processed PMMA/MWNT series. The data show that an increase in MWNT filler results in a systematic reduction in the peak intensity of tanδ and a modest overall positive shift in T_g. However, T_g shifts back downward slightly at the highest loading (3 wt%). The data also show systematic increases in the glassy and rubbery moduli with increasing loading, as expected. Similar to the melt mixed samples, the substantial decrease in tanδ intensity and the shift of both the glassy and rubbery moduli upward in the solution-based samples is a result of the nanotubes stiffening the polymer matrix. Yet, unlike the melt blended samples, the nanotubes in the solution-prepared samples show a significant effect on tanδ and the rubbery modulus at MWNT loadings as low as 0.2 wt%. This fact, coupled with the modest increase in T_g with increased loading suggests that some level of favorable interactions may be present between the polymer and the nanotubes.[10, 43] From direct visual observation during sample preparation it was discerned that the solution processing method was more effective at dispersing the nanotubes than melt mixing. The data supported this finding, in that reinforcement was apparent at much lower loadings in the solution processed samples.

Figure 4.6 shows the dielectric relaxations of the solution processed PMMA/MWNT samples at 30 Hz. The data reveal similar results as compared to the melt mixed samples. The β transition occurs at ~ 45°C while the α transition occurs at 117°C. However, the progressive increase in intensity with increasing loading that was seen in the melt mixed samples is not evident in the solution based samples. Also, the solution based samples appear to have a lower percolation threshold, as dielectric sweeps performed on the 0.3 wt% MWNT solution processed sample showed high levels of conduction. Solution prepared samples generally display better dispersion of the MWNT's due to the low viscosity of the solution during processing. Better dispersion is consistent with a lower percolation threshold, as the sample approaches a uniform, "theoretical" dispersion of nanotubes. Owing to the practical experimental constraint imposed by percolation, only the melt mixed samples and the solution processed samples described above were tested using BDS, as only a very limited range of sample loadings could be explored.

4.3.2.2 PMMA/MWNT-ox Composites

Thermogravimetric analysis results for the solution processed PMMA/MWNT-ox series are provided in **Table 4.3**. For these samples, the oxidized nanotubes were used. The table shows the preparation values and the measured values that were calculated using TGA results. Actual nanotube concentration was defined as any remaining material in a particular experimental run at 800°C minus the baseline at 800°C. Once again, the reported values and the actual values are very close to being identical; as such, samples will be identified according to their nominal loadings.

Figure 4.7 shows dynamic mechanical results for the solution processed PMMA/MWNT-ox series. The data show that an increase in MWNT-ox filler results in a systematic decrease in tanδ peak intensity and a substantial downward shift in T_g. The data also show an upward trend in both the glassy and rubbery moduli with increasing loadings, as expected. Also, as loading increases the recovery in the rubbery domain becomes less pronounced until at 3 wt% only a simple rubbery plateau is observed. Once again the increase in the glassy and rubbery moduli, and the substantial decrease of tanδ intensity, can be attributed to the stiffening effect of the nanotubes on the polymer

composite. Unique to this set of samples is the considerable downward shift of T_g displayed by the composites as loading increases. Previous observations from other nanocomposite systems suggest that unfavorable interactions or poor wetting between the polymer and the nanotubes may be responsible for the downward shift in T_g that is encountered.[74-75]

Figures 4.8a, **4.8b** and **4.8c** show comparisons of the dynamic mechanical modulus results for the PMMA/MWNT and PMMA/MWNT-ox samples for 0.5(a), 1.0(b) and 3.0 wt%(c), respectively. In these figures, it is possible to observe a significant reduction in T_g for the samples containing MWNT-ox nanotubes as compared to the untreated tubes. This can be explained by the fact that the procedure to oxidize the nanotubes also shortens the nanotubes thus allowing them to disperse easier and more uniformly. Previous studies have indicated that nanotubes which have been oxidized provide better dispersion within the polymer matrix but also decrease T_g, possibly due to poor wetting.[14, 36, 74-75]

Figures 4.9a, **4.9b** and **4.9c** show the tanδ dynamic mechanical results for the 0.5, 1.0 and 3.0 wt% PMMA/MWNT and PMMW/MWNT-ox solution processed composites, respectively. From these Figures it is possible to see the trend (i.e., lower T_g for MWNT-ox samples) across each set. **Table 4.4** contains the T_g of each sample, where the T_g value reported is taken as the peak in tanδ at 1 Hz. Visual observations during sample preparation showed that the composites with oxidized nanotubes had better solution dispersion characteristics, most likely due to shortened tube length (i.e., tubes shortened during nitric acid treatment). It is also possible that the carboxylic acid groups present on the oxidized tubes had a stronger affinity for DMF, thus allowing the tubes to disperse better. However, it appears that the oxidized tube surface, which is hydrophilic, is less compatible with PMMA. So, even though better tube dispersion is captured during the quenching process, the PMMA/MWNT-ox interaction is apparently less favorable and leads to a downward shift in T_g with increasing loading.

4.3.3 In-situ Polymerized Samples

4.3.3.1 Control Composites

Another method employed to disperse the nanotubes in the PMMA matrix was in-situ polymerization. In-situ polymerization was performed by free-radical thermal initiation within a suspension of MWNT's distributed in liquid methyl methacrylate monomer. An advantage of this method of preparation is the ability to distribute the nanotubes in the pre-polymerization blend which has a low viscosity. Recently it has been shown that the nanotubes, if functionalized appropriately, can participate in the polymerization reaction creating cross-links between the tubes and the polymer.[29-31] The disadvantage of using in-situ polymerization to produce nanocomposites is that free radicals present on the nanotubes can interfere with the polymerization reaction, decreasing the quality of the polymer matrix. In-situ polymerization also has an inherent disadvantage compared to the other methods in that the reaction itself contains many variables that must be precisely controlled in order to produce consistent composites (i.e. time, temperature, initiator concentration, agitation, etc.).

Up to this point, all synthesized samples have used commercial PMMA as the base polymer. However, to explore the interactions between functionalized nanotubes and the polymer more thoroughly, in-situ polymerization was performed. Dynamic Mechanical Analysis results for the unfilled PMMA control samples produced via each of the production methods (i.e., melt mixing, solution processing, in-situ polymerization) and commercial melt-pressed PMMA are shown in **Figure 4.10**. The control samples prepared via melt mixing and solution processing show good agreement with the commercial PMMA results and confirm that there are no significant changes in the commercial PMMA polymer when exposed to either Haake melt mixing or solution processing. The in-situ polymerized sample displays a comparable glassy modulus as compared to the commercial resin, and a somewhat greater rubbery modulus above the glass-rubber transition. However, the glass transition temperature for the in-situ polymerized sample is considerably lower (115°C vs. 130°C at 1Hz), and the transition is much broader as compared to the result for the commercial polymer. The lower T_g is most likely a reflection of a lower average degree of polymerization, with the breadth of

the relaxation suggesting higher polydispersity in the case of the in-situ polymerized specimen.

4.3.3.2 Optimization of In-situ Polymerization Parameters

Due to the number of variables that need to be controlled during the in-situ polymerization, an optimization process was undertaken. The main variables that were optimized for in-situ polymerization to produce PMMA were (i) polymerization time and temperature, (ii) initiator concentration, (iii) solvent content and (iv) amount of agitation during polymerization. The first factors to be optimized were polymerization time and temperature. These two factors had to be optimized in concert because polymerization rate is a strong function of temperature. Increasing the temperature of a reaction will reduce the amount of time needed for the monomer to completely polymerize.[27, 29] Also, increasing the temperature can increase auto-acceleration effects. Depending upon the synthesis conditions, PMMA polymerization can take anywhere from hours to weeks. In order to save time, a duration of 24 hours was chosen for the total polymerization time.[28] With a polymerization time established, it was possible to determine the optimum temperature for the reaction. Optimization of polymerization temperature began with a review of published articles that used MMA as the monomer and AIBN as the initiator. On this basis, it was determined that a temperature between 65 and 100^{o}C was desirable and a set of experiments was designed to clarify which temperature was optimal.[27-30, 40] After performing the polymerization at 5^{o}C intervals within the established range it was determined that 80^{o}C produced the best quality PMMA in the 24 hour period.

The next step in the optimization process was to determine the ideal amount of initiator for the reaction. The amount of AIBN was difficult to determine at the outset due to the wide range of values reported in previous studies. An increase in the amount of initiator can cause the polymer chains to be shorter, while a smaller amount of initiator would increase chain length but might not fully polymerize the samples within the 24 hour polymerization time. A set of samples varying in AIBN concentration from 0.10 to 0.35 wt% (based on MMA) were produced and the properties were assessed in order to ascertain the proper amount for polymerization of MMA. It was determined that a

concentration of 0.25 wt% AIBN relative to the MMA amount was needed for optimum results.

The presence of solvent in an in-situ polymerization reaction can lead to polymer chain termination and a reduction in potential auto-acceleration. For the nanocomposite samples prepared in this work, it was necessary to balance the need for solvent, in order to disperse the nanotubes, while at the same time maintaining the most favorable polymerization conditions. It was determined that solvent present in a 1:1 ratio with monomer provided the benefit of satisfactorily dispersing the nanotubes while still producing viable polymer.

Lastly, it was observed that two factors could greatly affect the quality of the synthesized polymer. The first was mechanical agitation due to stirring and sonication. Mechanical stirring was used in order to keep the nanotubes dispersed until the polymerization locked them into place. Sonication was also sometimes used instead of mechanical stirring to keep the nanotubes dispersed. However, the more agitation that was present (i.e. faster mechanical stirring), the worse the polymerization. This was also the case for the sonication. Polymer produced without sonication was of much higher quality than that produced when sonication was employed (based on visual and mechanical evaluation). Therefore, it was decided that the there would be no mechanical stirring or sonication so as to maximize the polymerization. The other factor that was found to affect polymerization was the amount of nanotubes present. The more nanotubes present in the pre-polymerization mixture, the worse the polymer produced. It was observed that samples with greater than ~ 5 wt% MWNT present in the mixture would not polymerize at all. This suggests that the nanotubes were interfering with the polymerization, either due to the increased viscosity of the pre-polymerization mixture or potential free radical quenching at the tube surface.

4.3.3.3 PMMA/MWNT-ox Composites

Thermogravimetric analysis was utilized in order to investigate the composition of the samples. **Figure 4.11** illustrates the TGA results for the in-situ polymerized PMMA/MWNT-ox set of composites ranging from the control up to 3 wt% MWNT-ox. The results of the TGA are interesting due to the dual decomposition events that are

visible. The first decomposition event begins around 300°C and accounts for about 20% of the total weight loss while the second event occurs around 400°C, and is consistent with the decomposition observed for the commercial PMMA. This behavior is probably a product of the wide range of molecular weight populations produced via the polymerization reaction. The dual weight loss character of the in-situ polymerized samples may reflect the decomposition of distinct molecular weight populations; the shorter polymer chains degrade at lower temperatures while the longer chains degrade across the same range as the commercial resin.

Figure 4.11 includes an expanded portion of the TGA results from 400 to 800°C. Actual nanotube concentration was defined as any remaining material in a given experiment at 800°C minus the baseline at 800°C. **Table 4.5** shows the target preparation values and the actual values that were determined based on the TGA tests. Overall, the measured values are modestly higher than the preparation values, potentially due to the loss of small amounts of unpolymerized monomer during sample preparation. For the sake of convenience, these samples will be referenced using their nominal loading (i.e. target) values throughout the rest of this section.

Dynamic mechanical results for the PMMA/MWNT-ox set of samples produced via in-situ polymerization are presented in **Figure 4.12**. The modulus results show the increase in stiffness with increasing loading in the rubbery domain, similar to the melt-mixed and solution-prepared composites. However, the loss results show no clear trend in T_g or tanδ peak intensity. The loss results (i.e. no to little change in T_g) seem to indicate that the nanotubes are not dispersing as consistently as was the case in the melt processed or solution processed samples. Due to the lack of mechanical stirring or sonication during the polymerization it is possible that the reaction is not occurring fast enough to "lock" the chains in place and the nanotubes are having time to clump back together. Nanotubes have often been discussed as having a potentially negative influence on polymerization reactions; e.g., increasing the viscosity of the pre-polymerization mixture, reducing mobility of the growing chains, as well as possible quenching reactions on the tube surface.

In order to verify that there is no clear trend in T_g for this set of composites, differential scanning calorimetry was performed and the results are presented in **Figure**

4.13. The T_g for a typical DSC experiment is defined as the midpoint of the transition on the heat flow curve. The samples containing nanotubes have approximately the same T_g as the control (within a few degrees), and there is no identifiable trend. This figure confirms the conclusion drawn from the dynamic mechanical results that there is no trend in T_g with increasing loading.

4.3.3.4 PMMA/MWNT-MMA Composites

Polymer grafting requires covalent functionalization of the surface of the nanotubes. The covalent functionalization can be achieved by direct addition of reagents to the nanotube wall or modification of the carboxylic acid groups already present on the oxidized nanotube surface. "Grafting to" and "grafting from" are the two strategies that have been reported for the covalent attachment of polymer to the nanotube. The "grafting from" strategy is the more popular of the two and is the one employed in this study. It involves the creation of initiation sites on the nanotube surface followed by polymerization of the polymer outward from the nanotube. Composites made via this technique can achieve very high grafting densities. Polymer grafting often involves the use of in-situ polymerization once the nanotube surface has been functionalized. Since polymer grafting also incorporates the use of in-situ polymerization in the production of composites, the same advantages and disadvantages of the polymerization method also apply to polymer grafting. The added benefit that polymer grafting should have over in-situ polymerization is that polymerization occurs from the functional group present on the surface thereby covalently linking the nanotube within the polymer matrix and thus maximizing the interfacial contact.

Since the results (above) suggested that the oxidized nanotubes were hindering the polymerization reaction, chemically functionalized nanotubes were incorporated into the polymerization study. The nanotubes were functionalized with a reactive methyl methacrylate group that would be likely to participate in the polymerization reaction (i.e. polymerization would occur from the functional group grafted to the nanotube surface).

Thermogravimetric analysis results for the PMMA/MWNT-MMA samples are illustrated in **Figure 4.14**. Much like the results obtained for the PMMW/MWNT-ox samples produced via in-situ polymerization, there is a dual decomposition evident in the

PMMA/MWNT-MMA composites. Since this feature is visible in all in-situ polymerized samples, even the control, it appears to be inherent to the in-situ polymerization. However, it is worth noting that the lower temperature decomposition effect becomes less intense with increased loading. This appears to indicate that the addition of the MWNT-MMA nanotubes could be helping to promote polymerization. **Figure 4.14** also shows an expanded portion of the results in the post-decomposition range above 600^{o}C. In this high temperature range the samples described above (i.e., nanocomposites based on commercial PMMA, etc) were stable at a constant weight up to 800^{o}C. In **Figure 4.14**, however, the measured weight continues to fall for all the samples loaded with nanotubes (expanded view). In addition, the composition of each individual sample in this temperature range is 3 to 5 times higher than was expected based on the initial target nanotube loading. This would appear to suggest that for some reason, residual polymer is persisting to much higher temperatures in these samples.

In order to determine if this result was an artifact of the TGA testing method (e.g., heating rate) a TGA experiment was performed by slowly heating the 1 wt% MWNT-MMA sample at 0.5^{o}C/min up to 350^{o}C in air. Then, at 350^{o}C, the atmosphere was changed to nitrogen and the sample was ramped at 20^{o}C/min up to 800^{o}C. The purpose of the slow heating in air was to allow ample time for any low molecular weight components to volatilize or decompose. The results from this TGA run are presented in **Figure 4.15**. The data give the impression that low molecular weight components are being provided ample time to exit the sample and are no longer present across the high temperature region. Thus, the composition in the high temperature region is much closer to the nominal preparation value of 1 wt% as compared to the original TGA experiment. This figure also shows that the low temperature portion of the curve no longer shows a dual decomposition character. Furthermore, the onset of weight loss occurs at lower temperature, although this is most likely due to the much lower heating rate.

Dynamic mechanical analysis was performed on the PMMA/MWNT-MMA composites and the results are displayed in **Figure 4.16**. All of the samples containing MWNT-MMA exhibit a modest increase in both the glassy modulus and the rubbery modulus, corresponding to a small increase in stiffness. The tanδ results reveal a significant increase in T_g with increased loading as well as a modest increase in tanδ

intensity at loadings of 0.5 wt% and 1.0 wt%. The increase in T_g with increasing loading is a sign that the functionalized nanotubes are interacting with the polymer in a favorable manner according to conventional composite theory.[10] Interestingly, the 0.2 wt% sample shows a dual T_g response. This is probably due to a wide range of molecular weights present in the composite. The dual T_g is not present in the 0.5 wt% and 1.0 wt% samples and it is apparent that the tanδ peaks get increasingly narrower with increased loading.

In order to verify the T_g results obtained from the DMA experiments, differential scanning calorimetry was performed on the PMMA/MWNT-MMA set of samples. Since the samples had shown evidence of dual T_g behavior, the DSC experiments were run under a heat/cool/heat cycle in order to probe the nature of the two populations. **Figure 4.17** shows the results of the DSC experiments. The top curve for each sample corresponds to the second heating cycle while the bottom curve for each sample corresponds to the first heating cycle. As expected the first heating cycle of all the samples corresponded well with the T_g data obtained from the DMA experiments. The T_g of the control is much lower than the filled composites and the 0.2 wt% sample shows a dual T_g behavior. However, across the second sweep the 0.2 wt% sample only shows one T_g. The new T_g evident on the second heating of the 0.2 wt% sample is almost exactly between the two T_g's of the first heating cycle. This seems to suggest that there was incomplete polymerization of the 0.2 wt% MWNT-MMA sample and that the temperatures reached by the first heating cycle were high enough to allow the polymer chains to finish polymerizing. The curves for the 0.5 wt% and 1.0 wt% samples show no evidence of incomplete polymerization and the response for the second heating sweep for both samples is identical to that observed in their respective first sweep.

In the absence of nanotube surface functionalization, the in-situ polymerization route did not appear to produce significant improvements in overall nanocomposite performance, with numerous potential complications owing to polymerization variables and potential tube agglomeration. On the other hand, the PMMA/MWNT-MMA samples show promise in improving some properties of the polymer. There is an increase in both the rubbery and glassy modulus, and a moderate increase in T_g with increasing loading. In this case, it appears the functional groups present on the tubes (MMA) are the driving

force for the increase in T_g. Two factors are responsible for this shift in T_g: an increase in polymer-nanotube surface compatibility owing to the presence of the MMA units and a restriction of chain mobility due to covalent bonding of the tubes to the polymer matrix. To fully elucidate these contributions, additional research is required to confirm the formation of covalent bonds at the tube surface, and to establish the most effective functional form for the enhancement of bulk composite properties.

4.4 Conclusions

The formulation of PMMA enhanced with carbon nanotubes could produce great improvement in strength and ductility in fields where the polymer must endure harsh conditions. One key factor limiting the application of MWNT-filled PMMA is the development of processes to disperse the nanotubes in the composite without diminishing other important properties. Consequently, recent research has focused on production methods that are able to adequately distribute the nanotubes within the polymer matrix. This thesis has focused on the characterization of a series of MWNT filled PMMA composites made via three different methods: melt mixing (PMMA/MWNT), solution processing (PMMA/MWNT, PMMA/MWNT-ox) and in-situ polymerization (PMMA/MWNT-ox, PMMA/MWNT-MMA). Samples were characterized using dynamic mechanical analysis, broadband dielectric spectroscopy, thermogravimetric analysis and differential scanning calorimetry. The goal was to gain a fundamental understanding of the polymer-filler interactions in these materials and their ultimate effect on macro-scale properties of the composite. The specific conclusions of this work are presented below.

Melt Mixed (PMMA/MWNT)

The relaxation dynamics of PMMA/MWNT composites have been examined using dynamic mechanical analysis. The inclusion of increasing amounts of nanotubes into the PMMA network increased both the glassy and rubbery modulus, but caused no change in the glass transition temperature. The results indicate that the melt mixing process is a viable method to disperse nanotubes within the polymer matrix, but there appears to be little interaction occurring at the polymer/filler interface.

The molecular dynamics of PMMA/MWNT composites were investigated using broadband dielectric spectroscopy. Two motional processes, β and α, were detected with increasing temperature. The dielectric intensity of the PMMA/MWNT samples made via melt mixing increased for both motional processes with increasing loading. Also, it was determined that nanotube filled PMMA composites show a percolation threshold occurring between 0.3 and 0.4 wt% MWNT owing to the conductive character of the nanotubes.

Solution Processed (PMMA/MWNT, PMMA/MWNT-ox)

Dynamic mechanical analysis has also been used to investigate the relaxation dynamics of PMMA/MWNT and PMMA/MWNT-ox composites made via solution processing. Both sets of samples showed an increase in the stiffness across the glassy and rubbery domains, and a subsequent decrease in tanδ intensity with increased loading; the stiffening contribution of the nanotubes was evident at lower loadings as compared to the melt processed samples. The glass transition temperature of the PMMA/MWNT samples remained relatively unchanged throughout the series while the PMMA/MWNT-ox samples showed a substantial decrease in glass transition temperature. The oxidized nanotubes are generally shorter than the untreated nanotubes due to damage incurred during the acid exposure process. The difference in the response of the two sets of samples reflects the improved dispersion that is possible with the MWNT-ox filler and also the potential for increased interaction between the MWNT-ox tubes and PMMA owing to enhanced interfacial surface area. This leads to an overall decrease in T_g because the carboxylic acid groups present on the oxidized tubes are less compatible with PMMA.

The dielectric intensity of the PMMA/MWNT composites made via solution processing was unchanged with increasing loading; however it should be noted that the change in filler loading across the sample set was very small so a large effect was not anticipated. Once more, it was determined that nanotube filled PMMA composites show a percolation threshold occurring around 0.3 wt% MWNT. The percolation threshold of the solution processed samples was slightly lower than their melt mixed counterparts due to the better dispersion obtained with solution processed samples.

In-situ Polymerization (PMMA/MWNT-ox, PMMA/MWNT-MMA)

The viscoelastic characteristics of PMMA/MWNT-ox and PMMA/MWNT-MMA composites (in-situ polymerization) were investigated using dynamic mechanical analysis. Both sets of samples displayed increased stiffness in the rubbery domain with increasing loading. While the PMMA/MWNT-ox set showed no clear trend in the glass transition temperature or tanδ intensity, the PMMA/MWNT-MMA series showed a modest increase in the glass transition temperature. The results for the PMMA/MWNT-ox series indicate that competing mechanisms are occurring. Increasing the amount of nanotubes increased the stiffness of the polymer matrix. However, increasing the loading appeared to reduce the extent of polymerization. The results obtained for the PMMA/MWNT-MMA set are very promising. The increase in glass transition temperature indicates that the polymer and filler are interacting in a positive fashion. The results also indicate that polymerization could be occurring from the functional groups grafted onto the nanotubes. While these results are encouraging for the introduction of functionalized nanotubes via in-situ polymerization, more work is needed in order to verify the results determined in this study.

Numerous series of PMMA based nanocomposites containing a range of nanotube concentrations have been investigated and correlations between production method, nanotube modification and viscoelastic response have been established. The insight gained from the polymer-nanotube interface characteristics determined in this work could likely be used in order to devise a production method for PMMA with enhanced properties for demanding applications.

Table 4.1: TGA results for melt mixed PMMA/MWNT composites; preparation and measured loading values are indicated. Measured values were determined from TGA results using the unfilled control as a baseline.

Name	Preparation Value (wt%)	Measured Value (wt%)
0.2 wt% MWNT	0.20	0.26
0.5 wt% MWNT	0.50	0.57
1.0 wt% MWNT	1.00	1.05
3.0 wt% MWNT	3.00	3.05
5.0 wt% MWNT	5.00	5.02

Table 4.2: TGA results for solution processed PMMA/MWNT composites; preparation and measured loading values are indicated. Measured values were determined from TGA results using the unfilled control as a baseline.

Name	Preparation Value (wt%)	Measured Value (wt%)
0.2 wt% MWNT	0.20	0.19
0.5 wt% MWNT	0.50	0.58
1.0 wt% MWNT	1.00	0.94
3.0 wt% MWNT	3.00	2.91

Table 4.3: TGA results for solution processed PMMA/MWNT-ox composites; preparation and measured loading values are indicated. Measured values were determined from TGA results using the unfilled control as a baseline.

Name	Preparation Value (wt%)	Measured Value (wt%)
0.2 wt% MWNT	0.20	0.15
0.5 wt% MWNT	0.50	0.64
1.0 wt% MWNT	1.00	1.10
3.0 wt% MWNT	3.00	2.94

Table 4.4: DMA results for solution processed PMMA/MWNT and PMMA/MWNT-ox composites. Reported T_g values are taken from the peak of the tanδ curves for each sample at 1 Hz.

Sample	T_g of MWNT (^oC)	T_g of MWNT-ox (^oC)
0.5 wt%	129	126
1.0 wt%	130	121
3.0 wt%	125	111

Table 4.5: TGA results for in-situ polymerized PMMA/MWNT-ox composites; preparation and measured loading values are indicated. Measured values were determined from TGA results using the unfilled control as a baseline.

Name	Preparation Value (wt%)	Measured Value (wt%)
0.2 wt% MWNT-ox	0.20	0.56
0.5 wt% MWNT-ox	0.50	0.78
1.0 wt% MWNT-ox	1.00	1.08
2.0 wt% MWNT-ox	2.00	2.42
3.0 wt% MWNT-ox	3.00	3.61

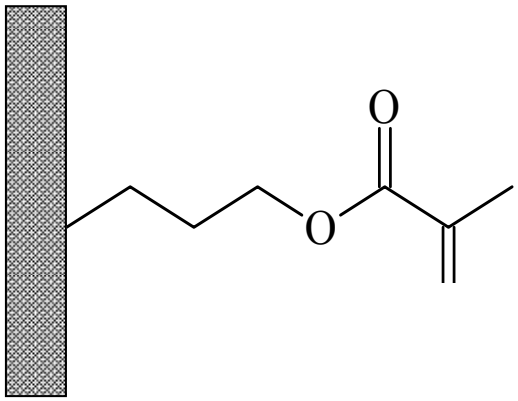

Figure 4.1: Schematic of methyl methacrylate functional group attached to surface of MWNT-MMA.

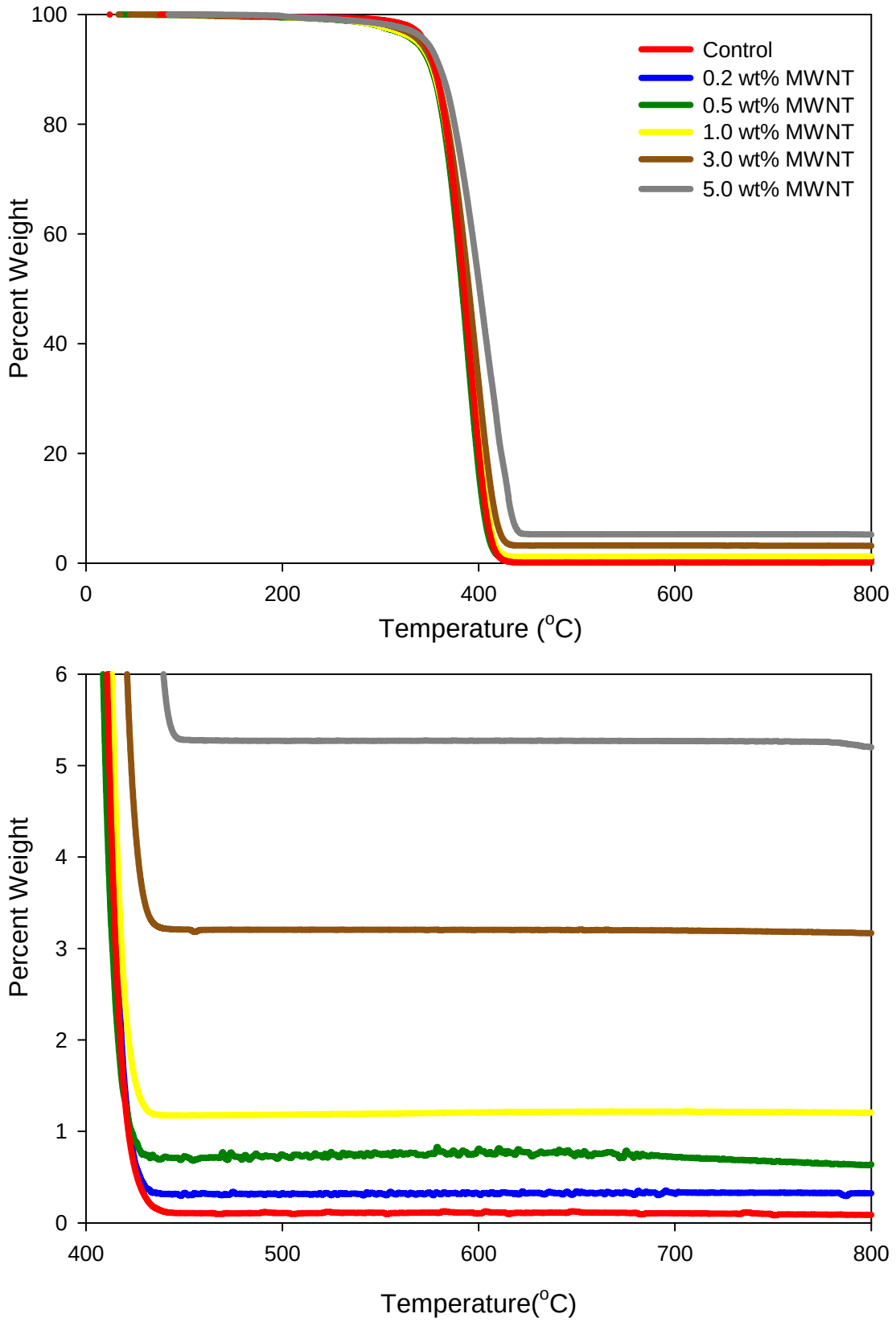

Figure 4.2: Thermogravimetric results for melt mixed samples: Percent weight (%) versus temperature. Heating rate of 20°C/min.

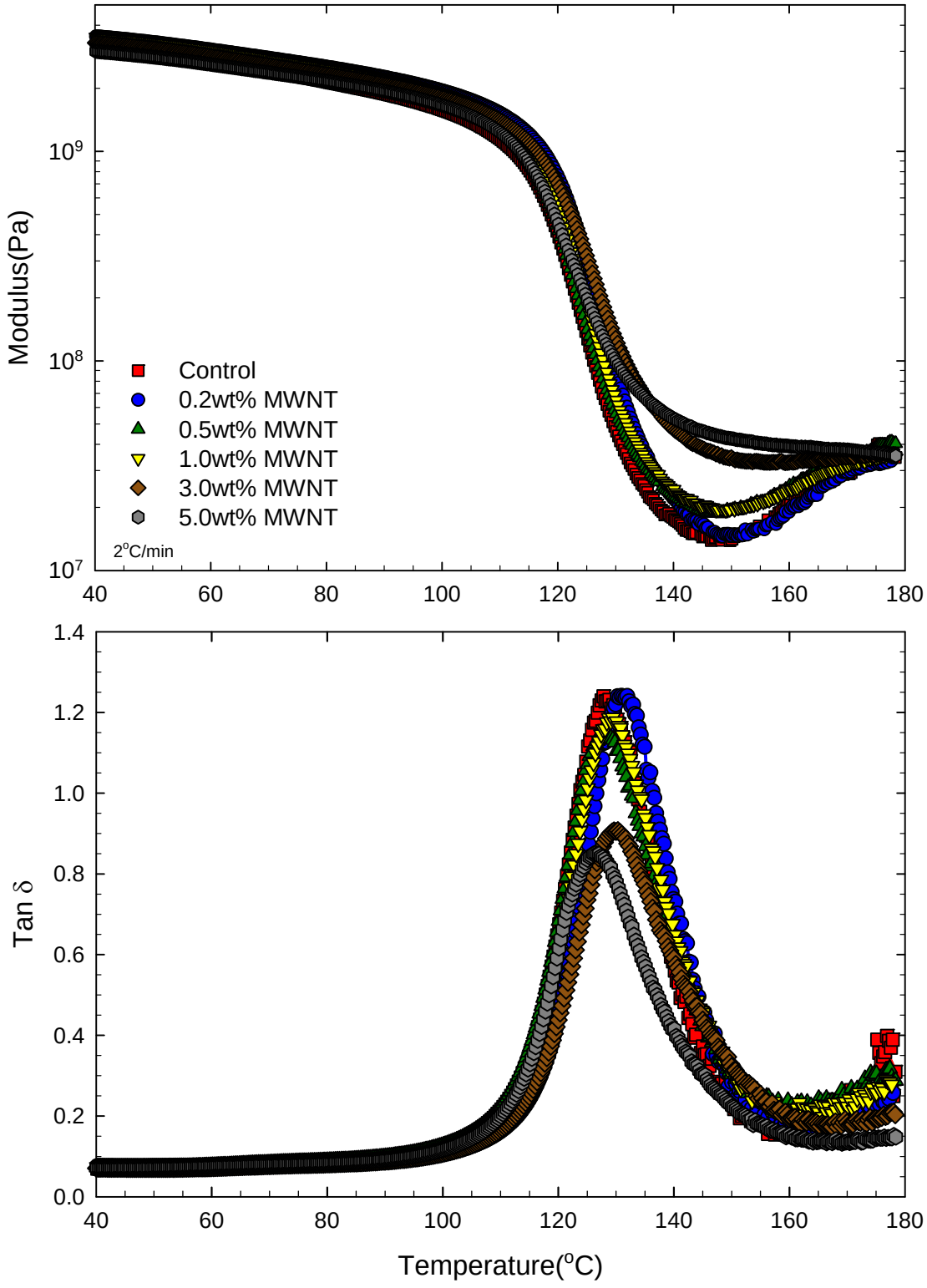

Figure 4.3: Dynamic mechanical results for melt mixed PMMA/MWNT composites: storage modulus (E') and loss factor (tanδ) versus temperature. Heating rate of 2°C/min

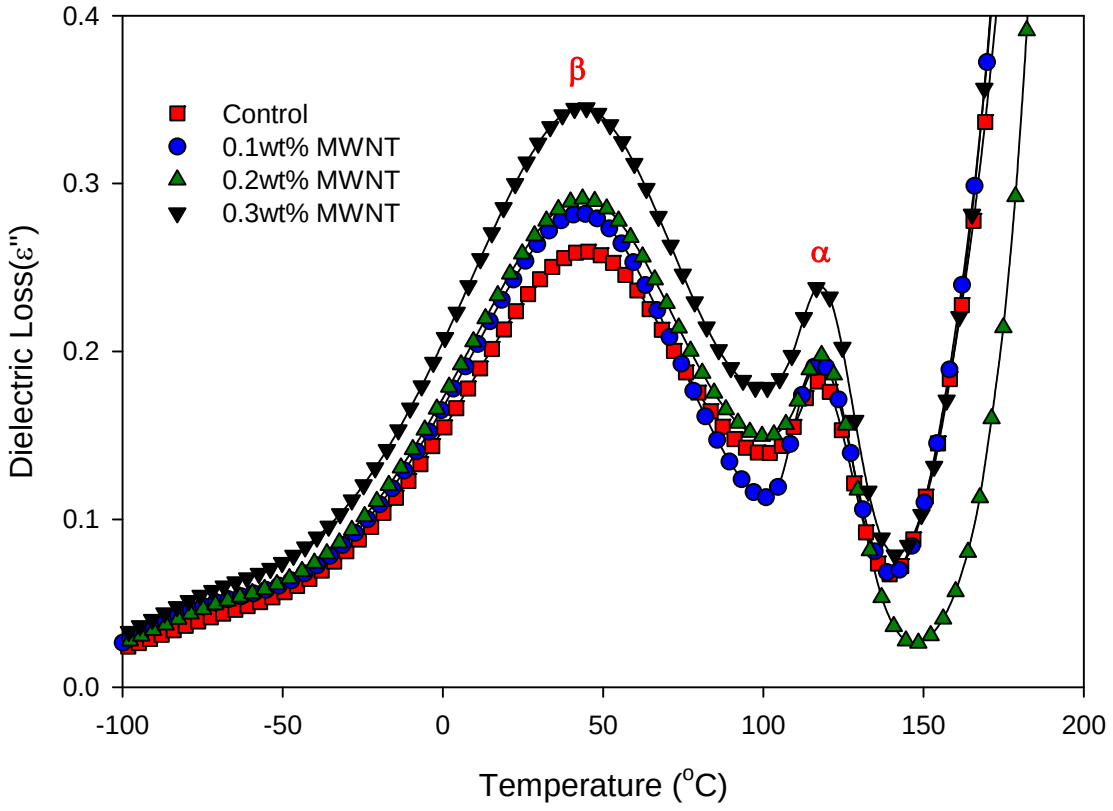

Figure 4.4: Dielectric Loss versus temperature for melt mixed PMMA/MWNT composites at 30 Hz.

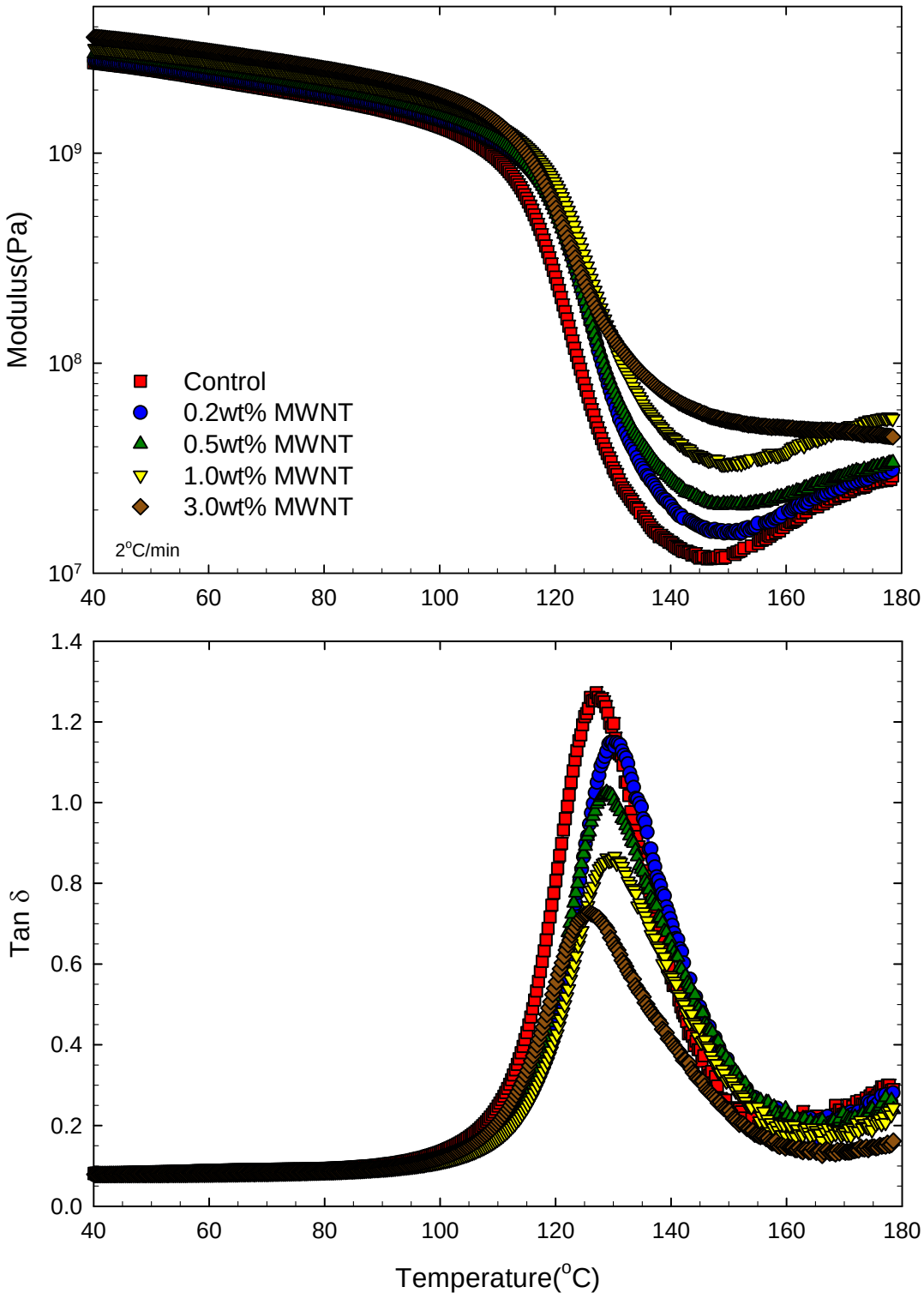

Figure 4.5: Dynamic mechanical results for solution processed PMMA/MWNT composites: storage modulus (E') and loss factor (tanδ) versus temperature. Heating rate of 2°C/min.

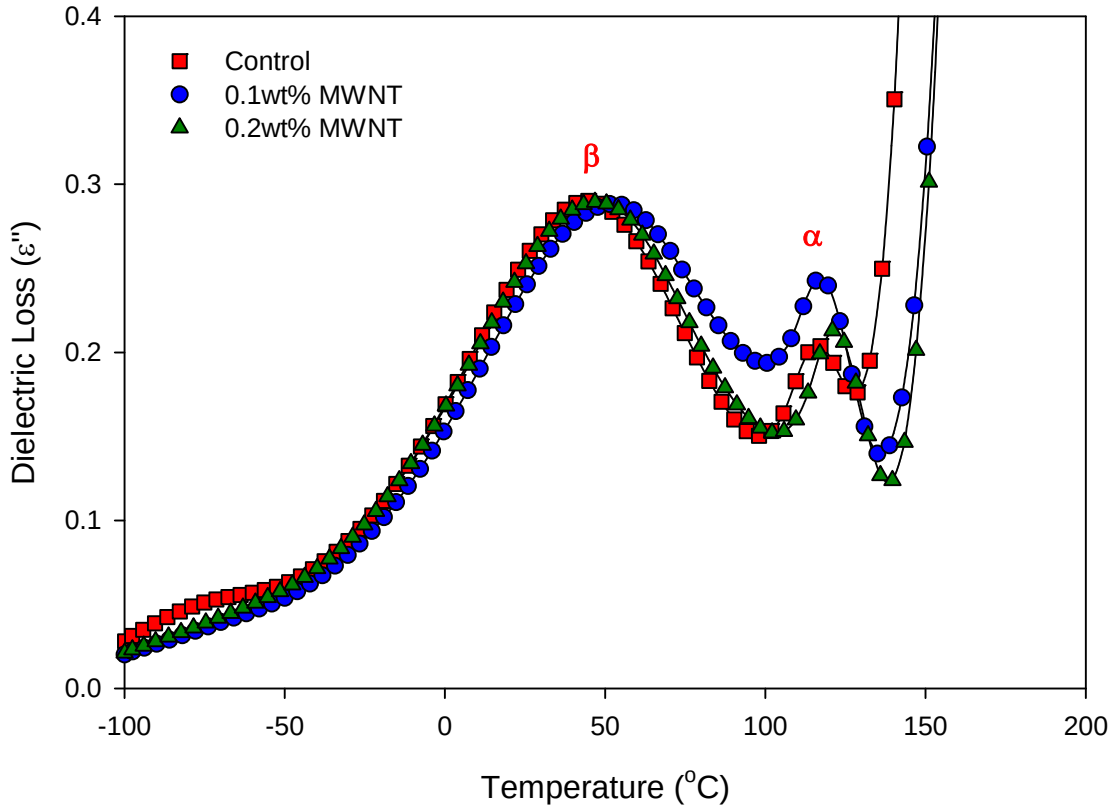

Figure 4.6: Dielectric loss versus temperature for solution processed PMMA/MWNT composites at 30 Hz.

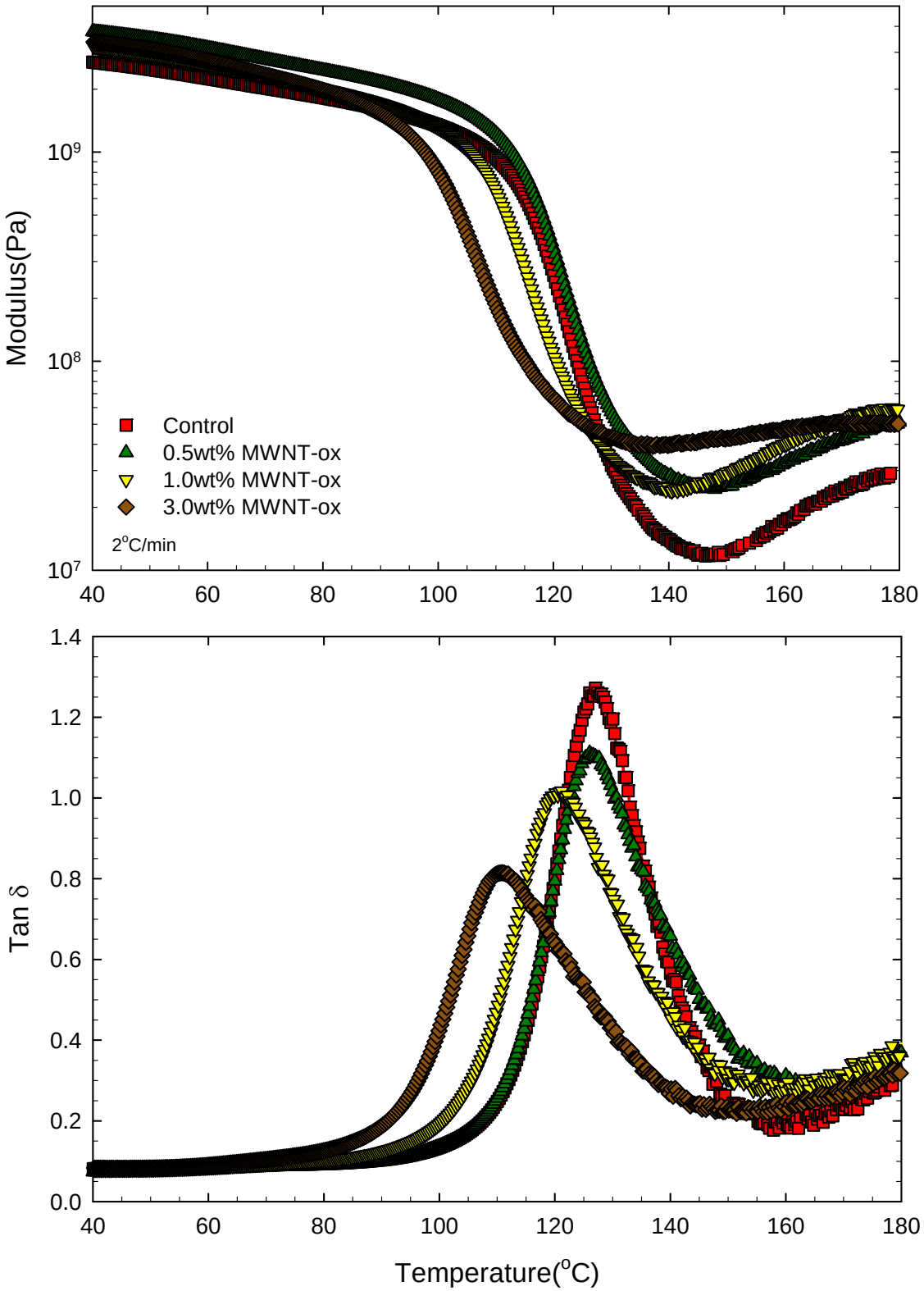

Figure 4.7: Dynamic mechanical results for solution processed PMMA/MWNT-ox composites: storage modulus (E') and loss factor (tanδ) versus temperature. Heating rate of 2°C/min.

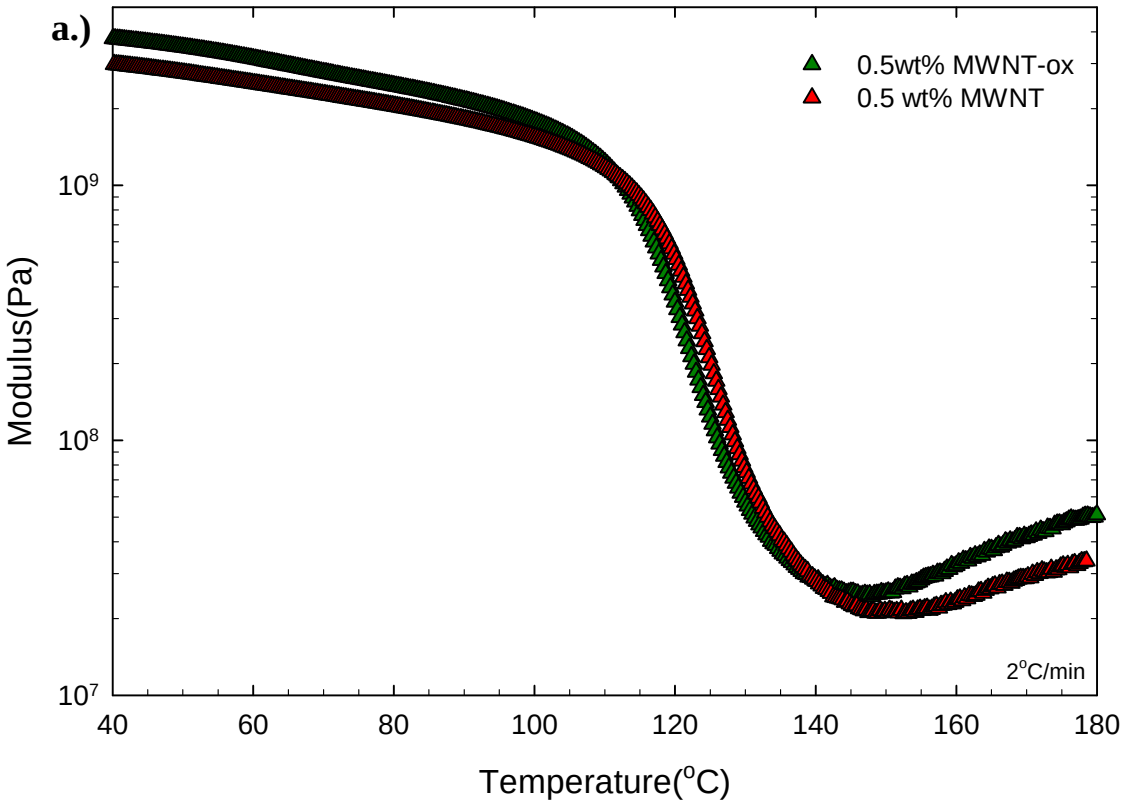
a.)
0.5wt% MWNT-ox
0.5 wt% MWNT
Modulus(Pa)
10^9
10^8
10^7
2°C/min
40
60
80
100
120
140
160
180
Temperature(°C)

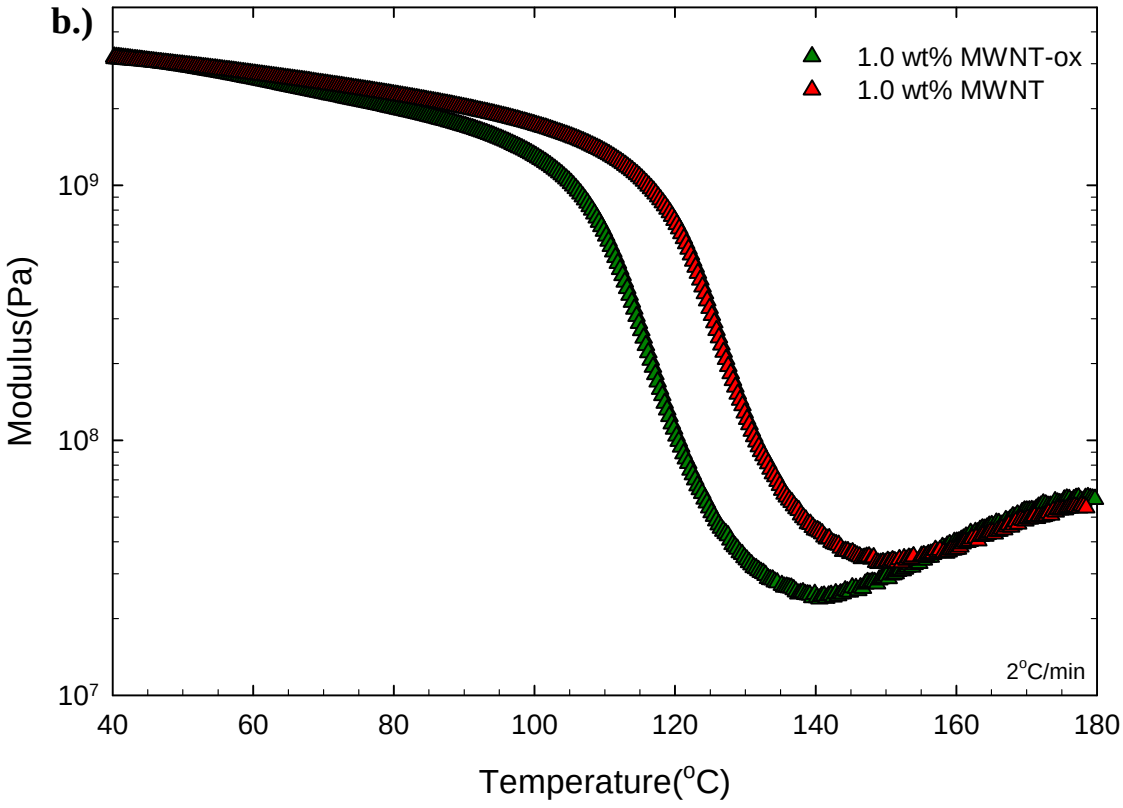
b.)
1.0 wt% MWNT-ox
1.0 wt% MWNT
Modulus(Pa)
10^9
10^8
10^7
2°C/min
40
60
80
100
120
140
160
180
Temperature(°C)

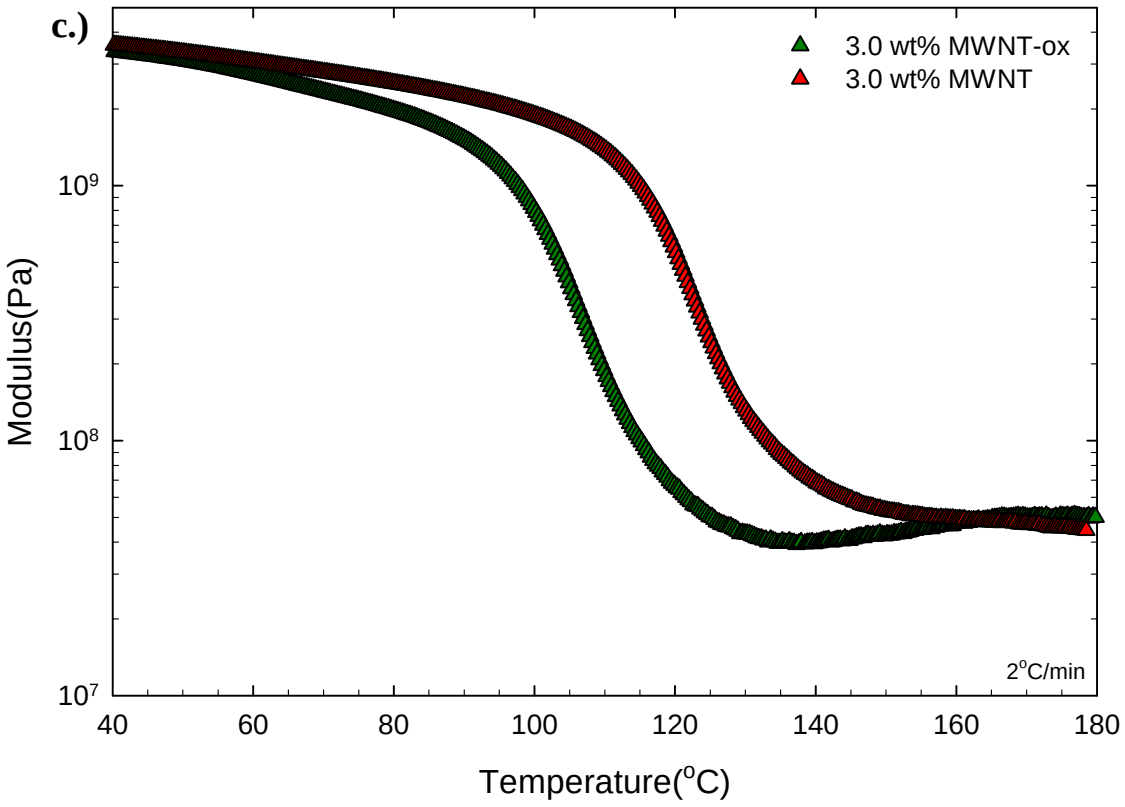

Figure 4.8: Dynamic mechanical results for solution processed samples containing 0.5(a), 1.0(b) and 3.0(c) wt% MWNT and MWNT-ox: storage modulus (E') versus temperature. Heating rate of 2°C/min.

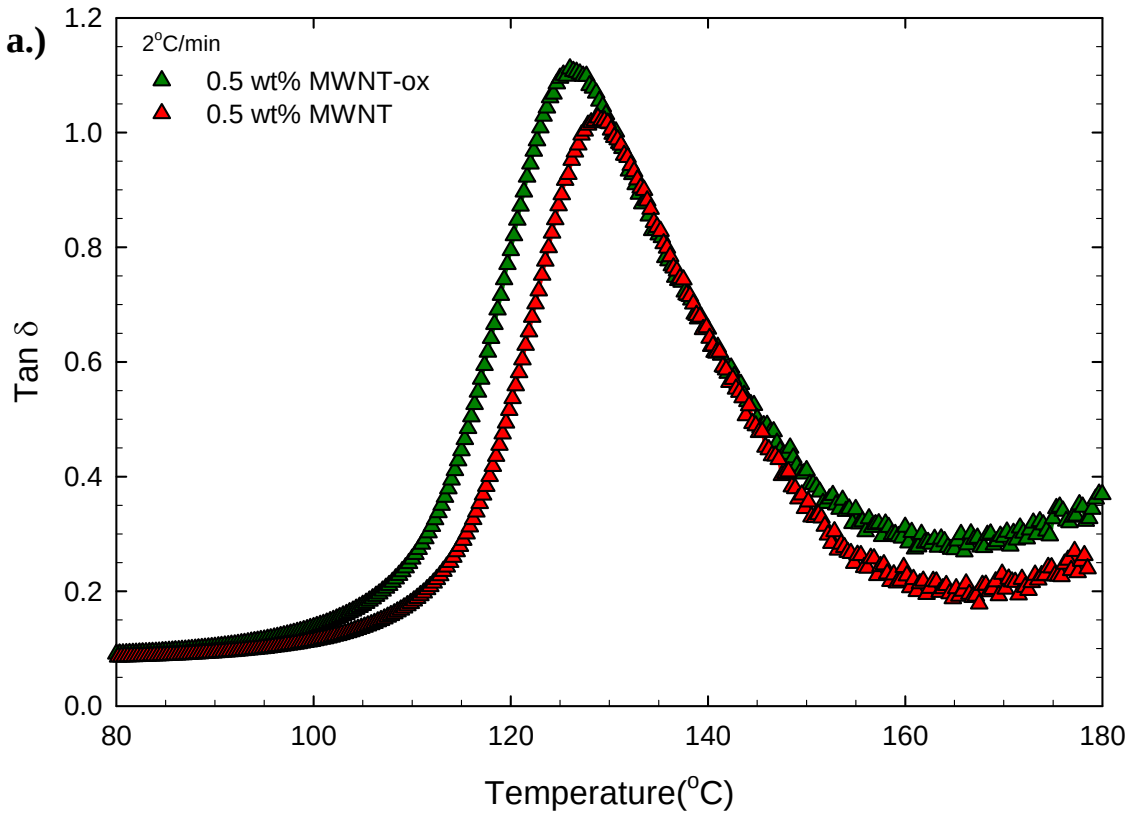
a.)
2°C/min
0.5 wt% MWNT-ox
0.5 wt% MWNT
Tan δ
Temperature(°C)
0.0
0.2
0.4
0.6
0.8
1.0
1.2
80
100
120
140
160
180

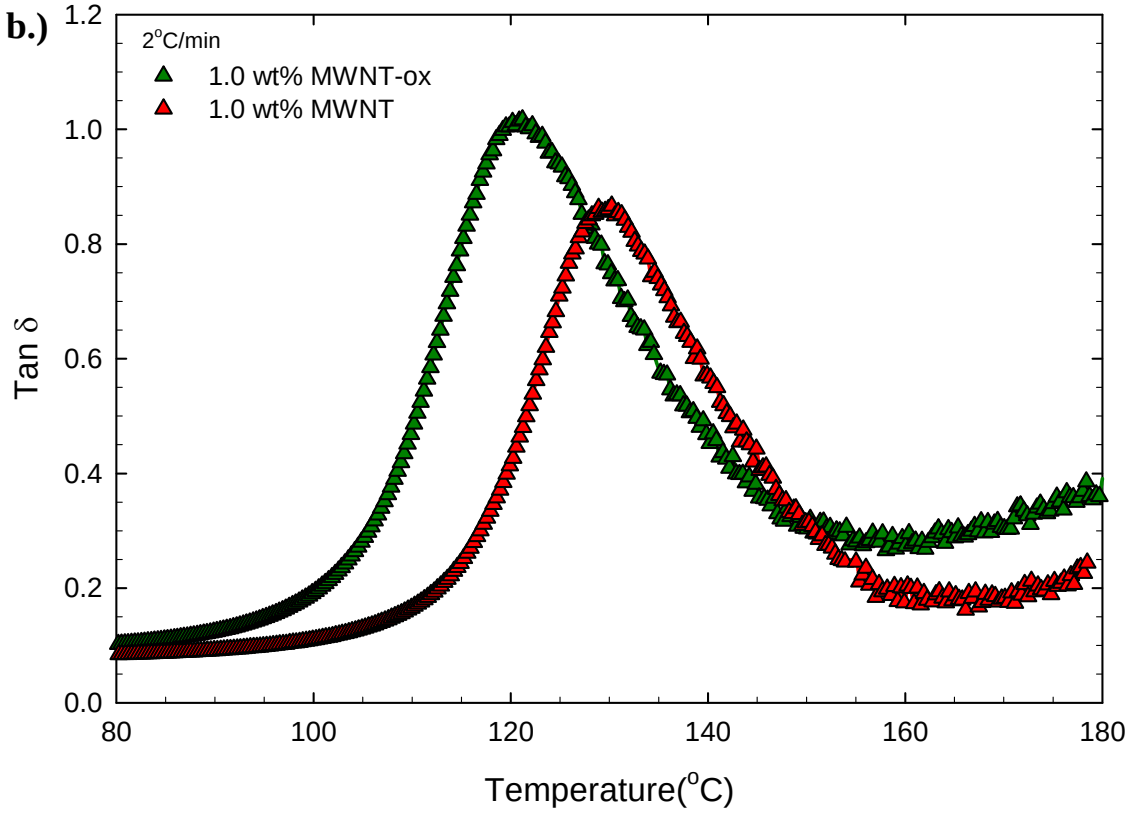
b.)
2°C/min
1.0 wt% MWNT-ox
1.0 wt% MWNT
Tan δ
Temperature(°C)
0.0
0.2
0.4
0.6
0.8
1.0
1.2
80
100
120
140
160
180

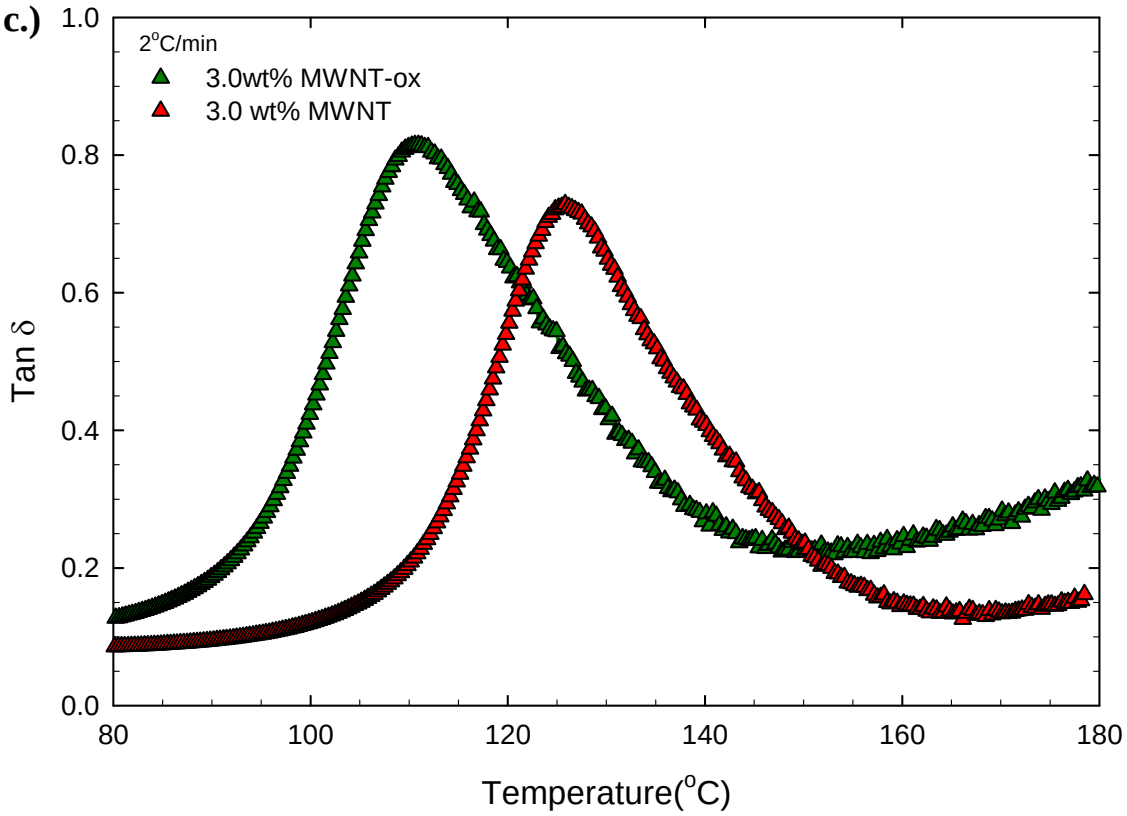

Figure 4.9: Dynamic mechanical results for solution processed samples containing 0.5(a), 1.0(b) and 3.0(c) wt% MWNT and MWNT-ox: loss factor (tanδ) versus temperature. Heating rate of 2°C/min.

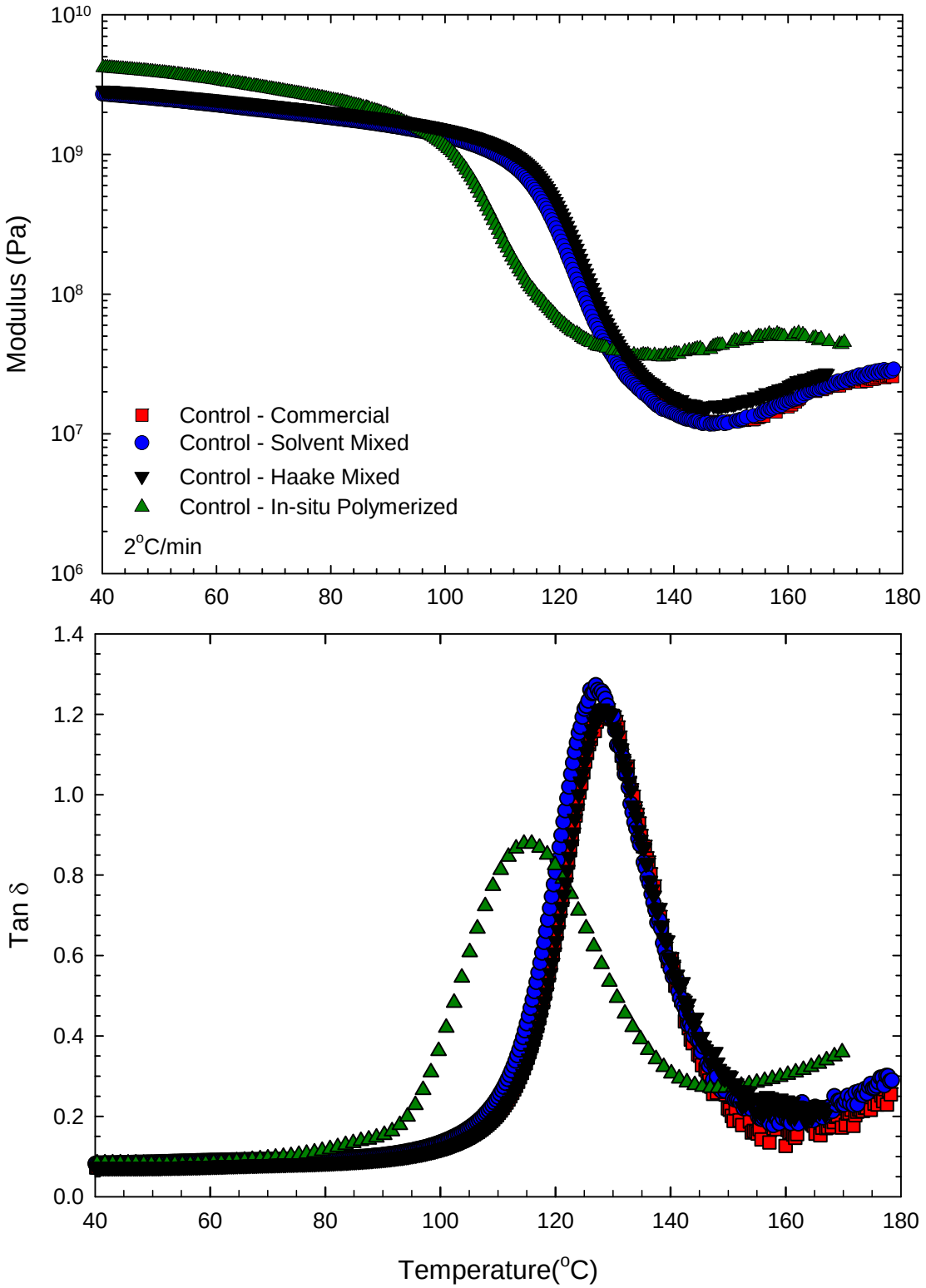

Figure 4.10: Dynamic mechanical results for unfilled PMMA control samples produced via melt mixing, solution processing, in-situ polymerization, as well as melt-pressed commercial PMMA: storage modulus (E') and loss factor (tanδ) versus temperature. Heating rate of 2°C/min.

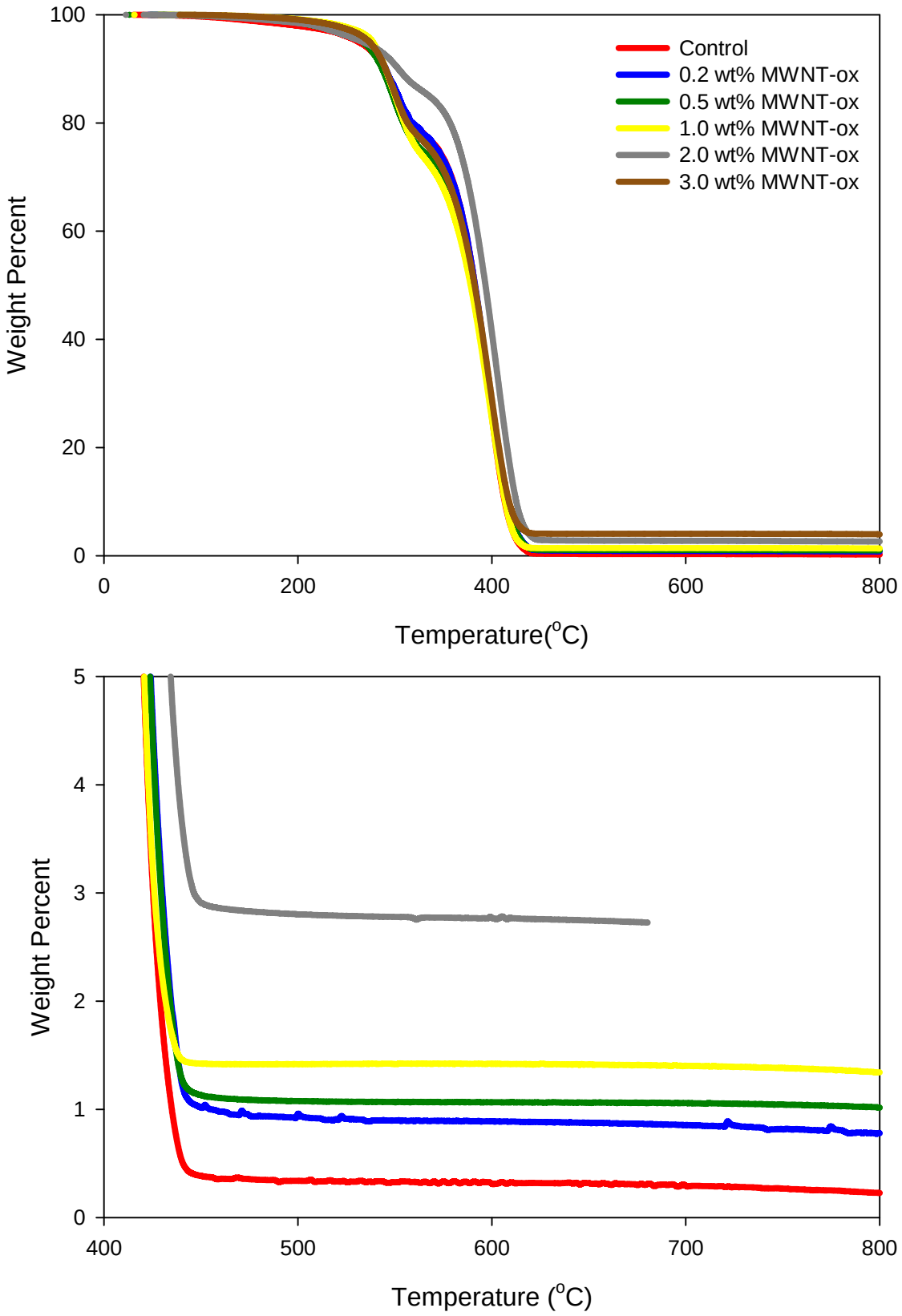

Figure 4.11: Thermogravimetric results for in-situ polymerized samples containing PMMA/MWNT-ox: Percent weight (%) versus temperature. Heating rate of 20°C/min.

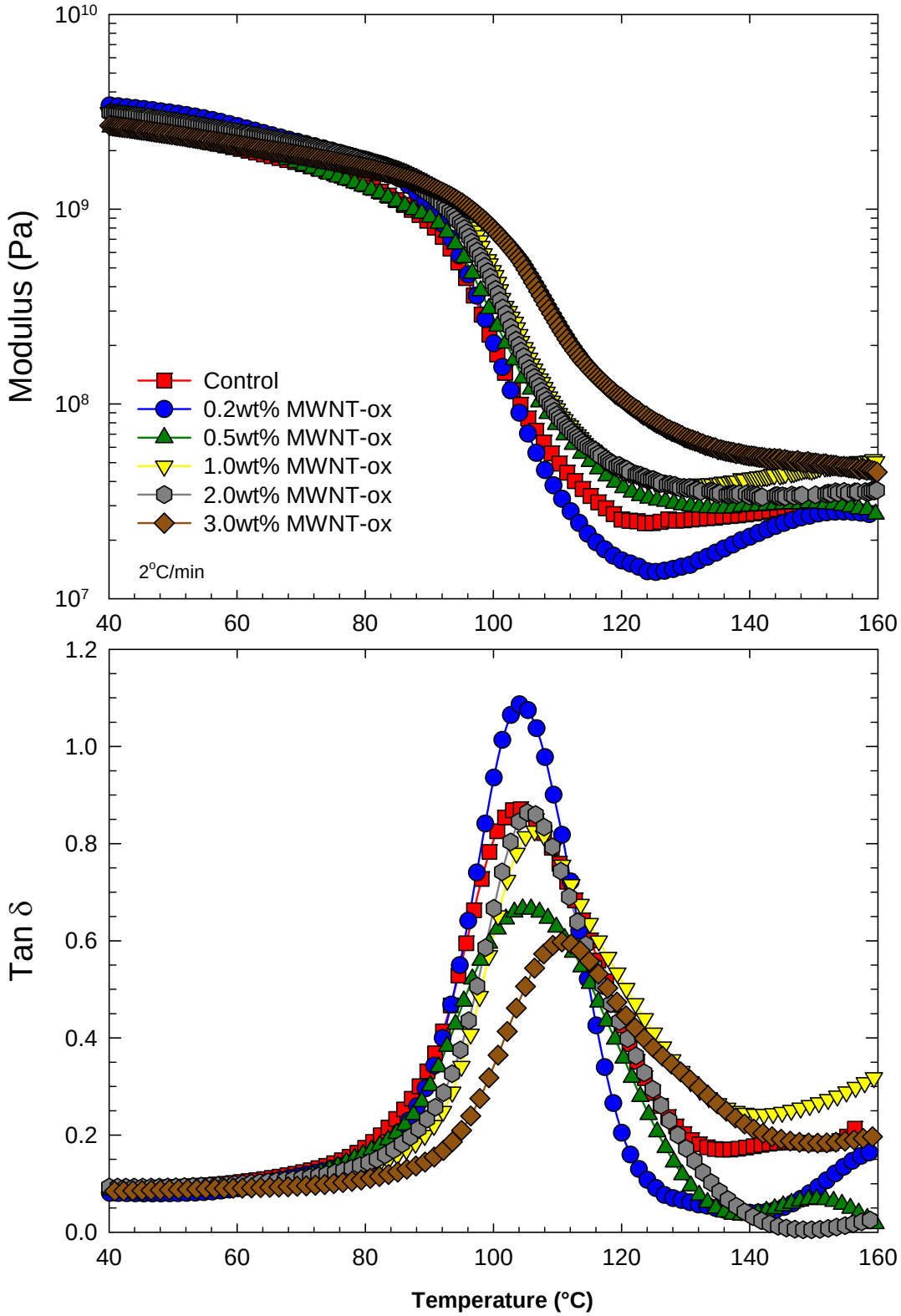

Figure 4.12: Dynamic mechanical results for PMMA/MWNT-ox composites produced via in-situ polymerization: storage modulus (E') and loss factor (tanδ) versus temperature. Heating rate of 2°C/min.

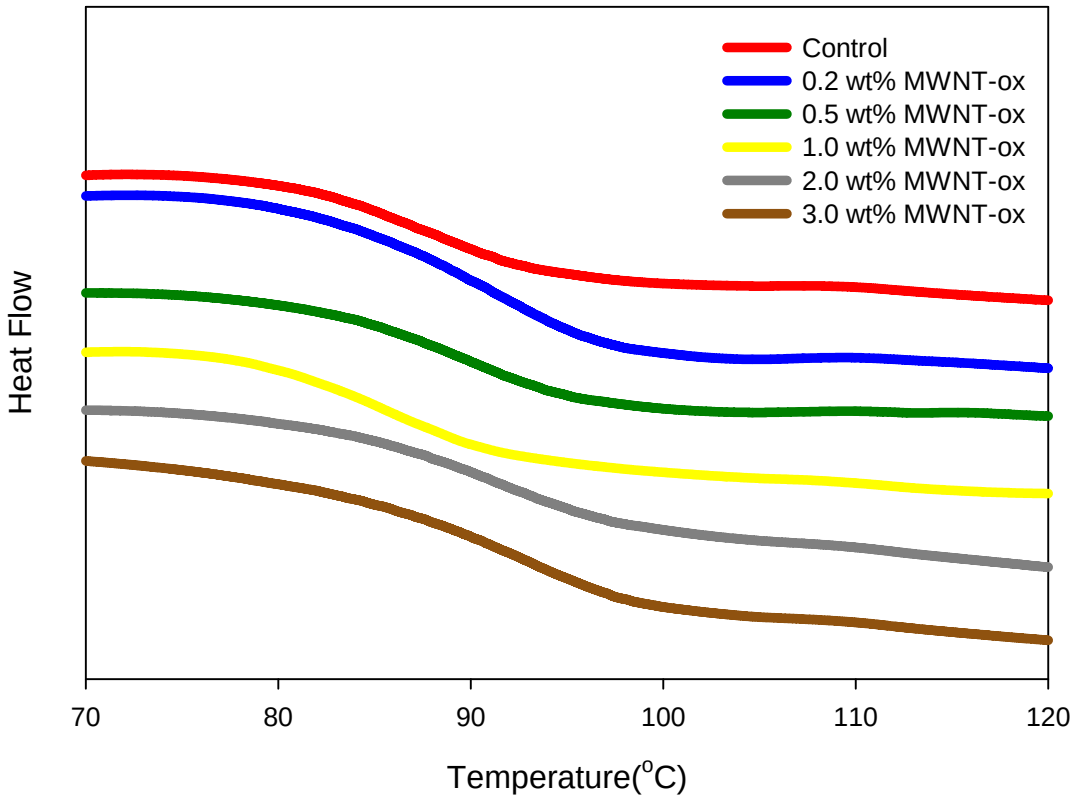

Figure 4.13: Differential scanning calorimetry results for PMMA/MWNT-ox composites produced via in-situ polymerization. Heat flow versus temperature. Heating rate of 10°C/min.

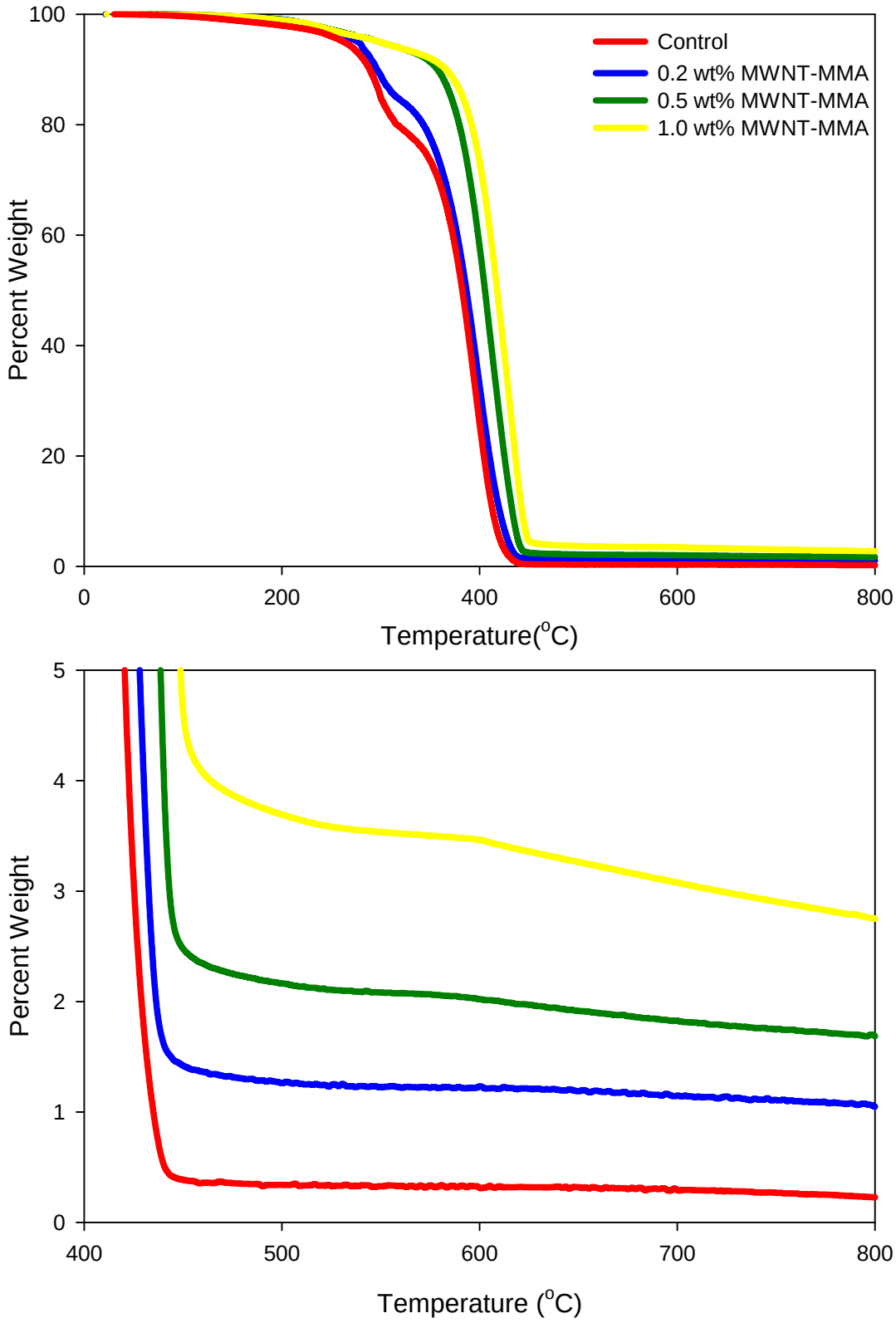

Figure 4.14: Thermogravimetric results for PMMA/MWNT-MMA composites produced via in-situ polymerization: Percent weight (%) versus temperature. Heating rate of 20°C/min.

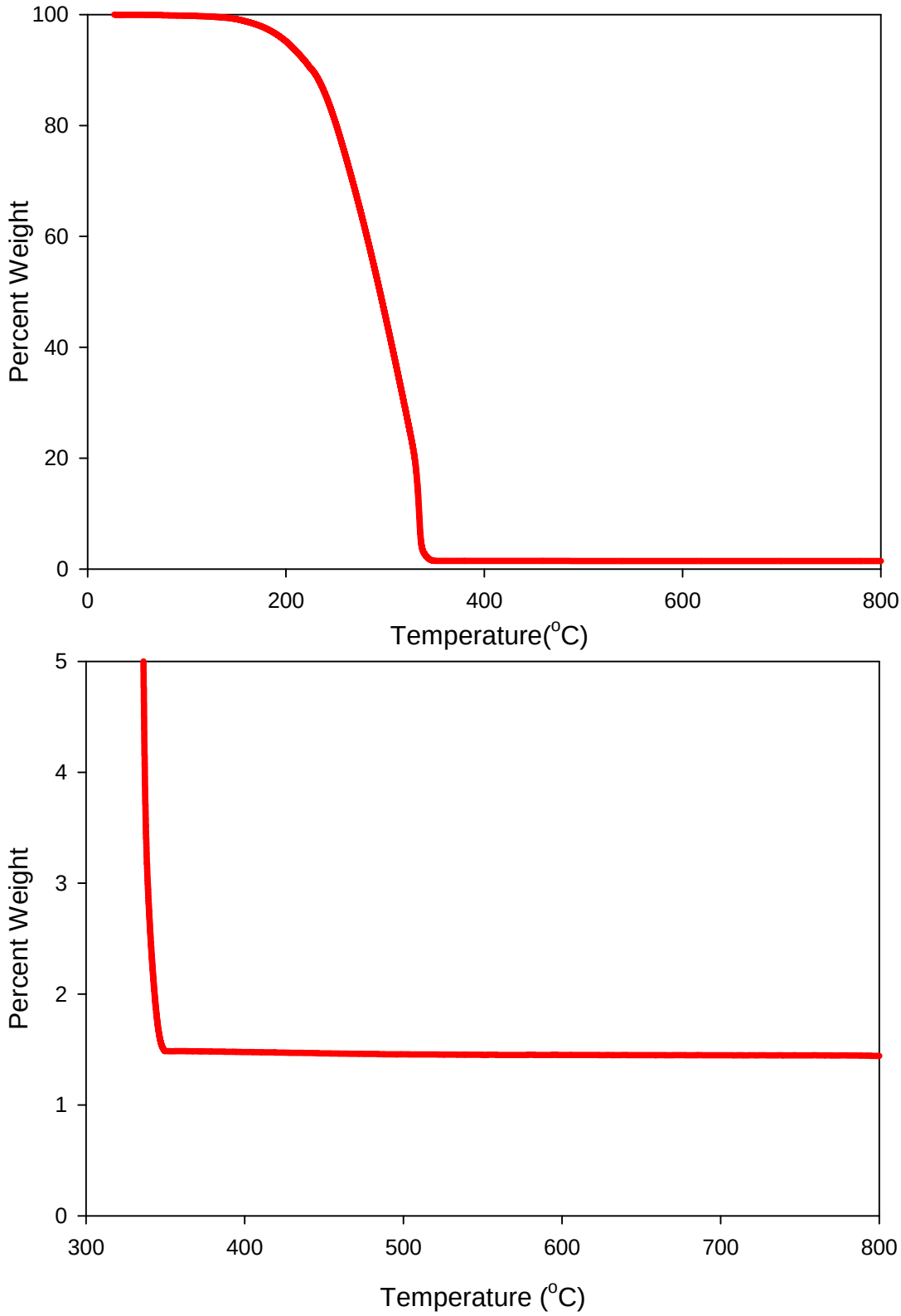

Figure 4.15: Thermogravimetric results for the 1 wt% MWNT-MMA sample produced via in-situ polymerization. Percent weight (%) versus temperature. Heating rate of 0.5°C/min up to 350°C then 20°C/min to 800°C.

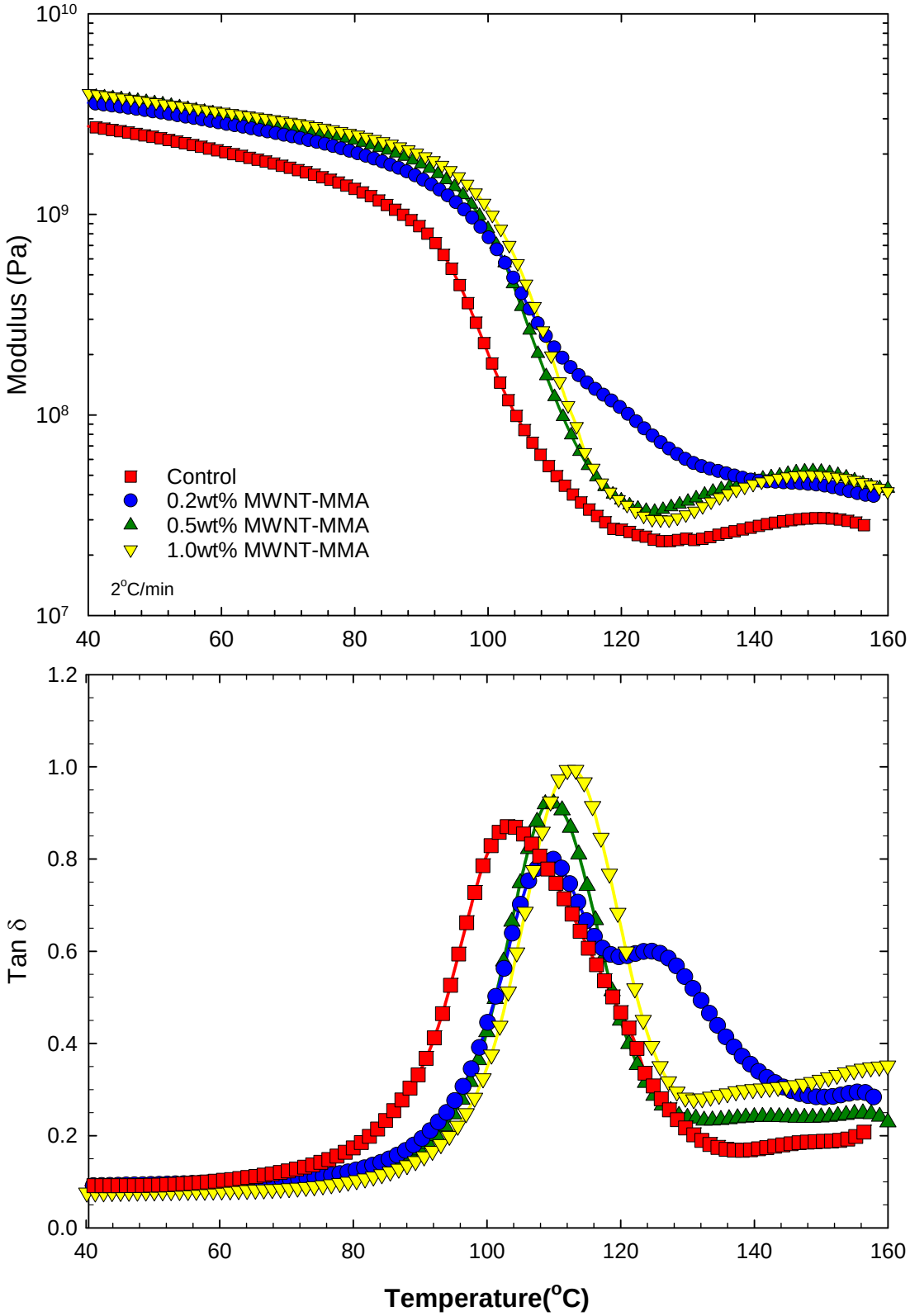

Figure 4.16: Dynamic mechanical results for PMMA/MWNT-MMA composites produced via in-situ polymerization: storage modulus (E') and loss factor (tanδ) versus temperature. Heating rate of 2°C/min

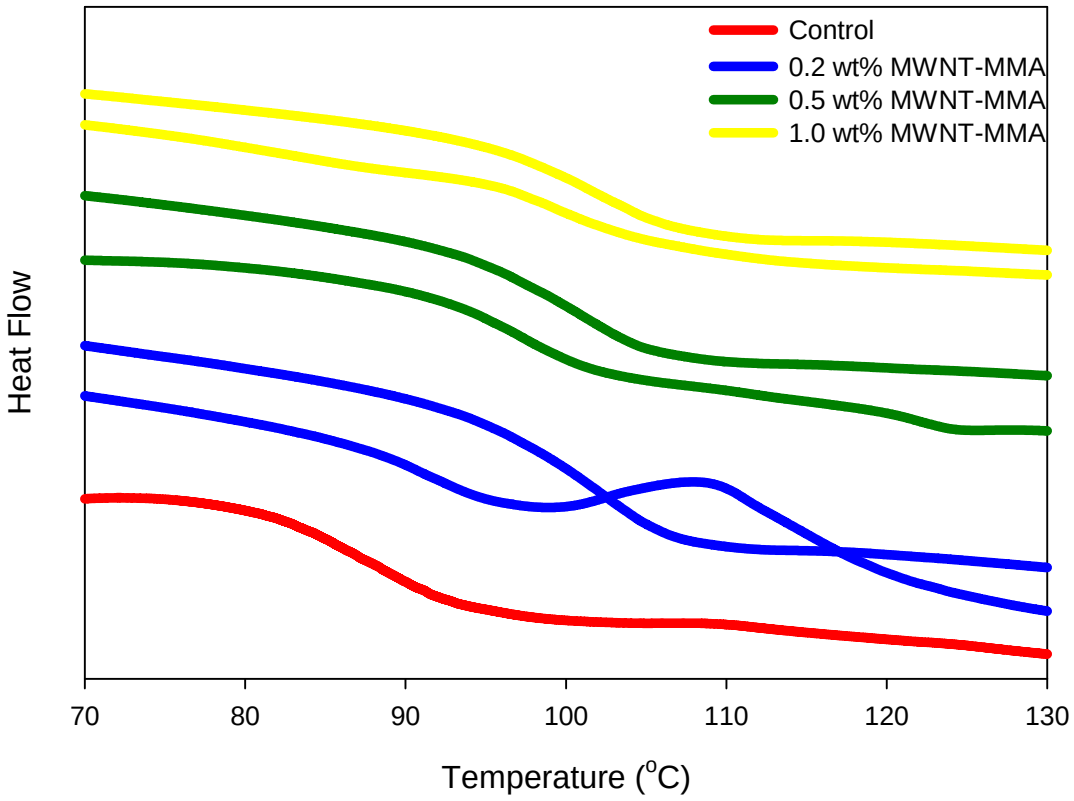

Figure 4.17: Differential scanning calorimetry results for PMMA/MWNT-MMA composites produced via in-situ polymerization. The top response for each sample corresponds to the second heating cycle while the bottom response for each sample corresponds to the first heating cycle. Heating rate of 10°C/min.

References

1. Moniruzzaman, M. and K.I. Winey, *Polymer Nanocomposites Containing Carbon Nanotubes.* Macromolecules, 2006. **39**: p. 5194-5205.
2. Xie, X.-L., Y.-W. Mai, and X.-P. Zhou, *Dispersion and Alignment of carbon nanotubes in polymer matrix: A review.* Materials Science and Engineering R, 2005. **49**: p. 89-112.
3. Coleman, J.N., U. Khan, and Y.K. Gun'ko, *Mechanical Reinforcement of Polymers Using Carbon Nanotubes.* Advanced Materials, 2006. **18**: p. 689-706.
4. Jin, Z., et al., *Poly(vinylidene fluoride)-assisted melt-blending of multi-walled carbon nanotube/poly(methyl methacrylate) composites.* Materials Research Bulletin, 2002. **37**: p. 271-278.
5. Li, Z.-M., et al., *A novel approach to preparing carbon nanotube reinforced thermoplastic polymer composites.* Carbon, 2005. **43**: p. 2397-2429.
6. Marrs, B., et al., *Augmentation of acrylic bone cement with multiwall carbon nanotubes.* Journal of Biomedical Materials Research, 2006. **77A**: p. 269-276.
7. Winey, K.I., R.A. Vaia, and G. Editors, *Polymer Nanocomposites.* MRS Bulletin, 2007. **32**: p. 314-322.
8. Jin, Z., et al., *Dynamic mechanical behavior of melt-processed multi-walled carbon nanotube/poly(methyl methacrylate) composites.* Chemical Physics Letters, 2001. **337**: p. 43-47.
9. Abdelrazek, E.M., *Physical properties of MgCl2-filled PMMA films for optical applications.* Physica B: Condensed Matter (Amsterdam, Netherlands), 2004. **351**(1-2): p. 83-89.
10. Schadler, L.S., et al., *Designed interfaces in polymer nanocomposites: a fundamental viewpoint.* MRS Bull., 2007. **32**(4): p. 335-340.
11. Krishnamoorti, R., *Strategies for Dispersing Nanoparticles in Polymers.* MRS Bulletin, 2007. **32**: p. 341-347.
12. Drzal, L.T., M.J. Rich, and P.F. Lloyd, *Adhesion of graphite fibers to epoxy matrices: I. The role of fiber surface treatment.* Journal of Adhesion, 1983. **16**(1): p. 1-30.
13. Rittigstein, P., et al., *Model polymer nanocomposites provide an understanding of confinement effects in real nanocomposites.* Nat Mater, 2007. **6**(4): p. 278-82.
14. Andrews, R. and M.C. Weisenberger, *Carbon nanotube polymer composites.* Curr. Opin. Solid State Mater. Sci., 2004. **8**(1): p. 31-37.
15. O'Connell, M.J., et al., *Reversible water-solubilization of single-walled carbon nanotubes by polymer wrapping.* Chem. Phys. Lett., 2001. **342**(3,4): p. 265-271.
16. Star, A., et al., *Preparation and properties of polymer-wrapped single-walled carbon nanotubes.* Angew. Chem., Int. Ed., 2001. **40**(9): p. 1721-1725.
17. Bansal, A., et al., *Quantitative equivalence between polymer nanocomposites and thin polymer films.* Nat Mater, 2005. **4**(9): p. 693-8.
18. Long, D. and P. Sotta, *How the shift of the glass transition temperature of thin polymer films depends on the adsorption with the substrate.* Los Alamos National Laboratory, Preprint Archive, Condensed Matter, 2003: p. 1-33.
19. Hartmann, L., et al., *Molecular dynamics in thin films of isotactic poly(methyl methacrylate).* European Physical Journal E: Soft Matter, 2002. **8**(2): p. 145-154.

20. Pham, J.Q. and P.F. Green, *The glass transition of thin film polymer/polymer blends: Interfacial interactions and confinement.* Journal of Chemical Physics, 2002. **116**(13): p. 5801-5806.
21. Haggenmueller, R., et al., *Aligned single-wall carbon nanotubes in composites by melt processing methods.* Chemical Physics Letters, 2000. **330**: p. 219-225.
22. Potschke, P., et al., *Melt Mixing as Method to Disperse Carbon Nanotubes into Thermoplastic Polymers.* Fullerenes, Nanotubes and Carbon Nanostructures, 2005. **13**: p. 211-224.
23. Liu, J., T. Liu, and S. Kumar, *Effect of solvent solubility parameter on SWNT dispersion in PMMA.* Polymer, 2005. **46**(10): p. 3419-3424.
24. Du, F., J.E. Fischer, and K.I. Winey, *Coagulation Method for Preparing Single-Walled Carbon Nanotube/Poly(methyl methacrylate) Composites and Their Modulus, Electrical Conductivity and Thermal Stability.* Journal of Polymer Science: Part B: Polymer Physics, 2003. **41**: p. 3333-3338.
25. Du, F., et al., *Nanotube networks in polymer nanocomposites: Rheology and electrical conductivity.* Macromolecules, 2004. **37**(24): p. 9048-9055.
26. Jia, Z., et al., *Study on poly(methyl methacrylate)/carbon nanotube composites.* Materials Science and Engineering, 1999. **A271**: p. 395-400.
27. Kim, S.T., et al., *Dispersion-Polymerized Carbon Nanotube/Poly(methyl methacrylate) Composite Particles and their Electrorheological Characteristics.* Macromolecular Chemistry and Physics, 2007. **208**: p. 514-519.
28. Park, S.J., et al., *Synthesis and Dispersion Characteristics of Multi-Walled Carbon Nanotube Composites with Poly(methyl methacrylate) Prepared by In-Situ Bulk Polymerization.* Macromolecular Rapid Communications, 2003(24): p. 1070-1073.
29. Putz, K.W., et al., *Elastic Modulus of Single-Walled Carbon Nanotube/Poly(methyl methacrylate) Nanocomposites.* Journal of Polymer Science: Part B: Polymer Physics, 2004. **42**: p. 2286-2293.
30. Raravikar, N.R., et al., *Synthesis and Characterization of Thickness-Aligned Carbon Nanotube-Polymer Composite Films.* Chemistry of Materials, 2005. **17**(974-983).
31. Velasco-Santos, C., et al., *Improvement of Thermal and Mechanical Properties of Carbon Nanotube Composites through Chemical Functionalization.* Chemistry of Materials, 2003. **15**: p. 4470-4475.
32. Hu, Y., S. Zhou, and L. Wu, *Surface mechanical properties of transparent poly(methyl methacrylate)/zirconia nanocomposites prepared by in situ bulk polymerization.* Polymer, 2009. **50**: p. 3609-3616.
33. Kang, X., et al., *Vinyl-Carbon Nanotubes for Composite Polymer Materials.* Journal of Applied Polymer Science, 2008. **110**: p. 1915-1920.
34. Kong, H., C. Gao, and D. Yan, *Controlled functionalization of multiwalled carbon nanotubes by in situ atom transfer radical polymerization.* J Am Chem Soc, 2004. **126**(2): p. 412-3.
35. Qin, S., et al., *Polymer brushes on single-walled carbon nanotubes by atom transfer radical polymerization of n-butyl methacrylate.* J. Am. Chem. Soc., 2004. **126**(1): p. 170-176.

36. Andrews, R., et al., *Multiwall Carbon Nanotubes: Synthesis and Application.* Acc. Chem. Res., 2002. **35**(12): p. 1008-1017.
37. Haggenmueller, R., et al., *Production and characterization of polymer nanocomposites with highly aligned single-walled carbon nanotubes.* Journal of Nanoscience and Nanotechnology, 2003. **3**(1/2): p. 105-110.
38. Zhu, J., et al., *Reinforcing epoxy polymer composites through covalent integration of functionalized nanotubes.* Advanced Functional Materials, 2004. **14**(7): p. 643-648.
39. Cadek, M., et al., *Morphological and mechanical properties of carbon-nanotube-reinforced semicrystalline and amorphous polymer composites.* Applied Physics Letters, 2002. **81**(27): p. 5123-5125.
40. Velasco-Santos, C., et al., *Dynamical-mechanical and thermal analysis of carbon nanotube-methyl-ethyl methacrylate nanocomposites.* Journal of Physics D: Applied Physics, 2003. **36**(12): p. 1423-1428.
41. Cadek, M., et al., *Reinforcement of Polymers with Carbon Nanotubes: The Role of Nanotube Surface Area.* Nano Letters, 2004. **4**(2): p. 353-356.
42. Meincke, O., et al., *Mechanical properties and electrical conductivity of carbon-nanotube filled polyamide-6 and its blends with acrylonitrile/butadiene/styrene.* Polymer, 2004. **45**(3): p. 739-748.
43. Liu, T., et al., *Morphology and mechanical properties of multiwalled carbon nanotubes reinforced nylon-6 composites.* Macromolecules, 2004. **37**(19): p. 7214-7222.
44. Zhang, W.D., et al., *Carbon Nanotubes Reinforced Nylon-6 Composite Prepared by Simple Melt-Compounding.* Macromolecules, 2004. **37**(2): p. 256-259.
45. Hwang, G.L., Y.-T. Shieh, and K.C. Hwang, *Efficient load transfer to polymer-grafted multiwalled carbon nanotubes in polymer composites.* Advanced Functional Materials, 2004. **14**(5): p. 487-491.
46. Kanapitsas, A., et al., *Study on electrical/dielectric and thermomechanical properties of polymer-carbon nanotubes nanocomposites.* Recent Advances in Nanotechnology, Proceedings of the WSEAS International Conference on Nanotechnology, 1st, Cambridge, United Kingdom, Feb. 21-23, 2009, 2009: p. 75-81.
47. Pandis, C., et al., *Thermal and electrical characterization of polypropylene/carbon nanotube nanocomposites.* NSTI Nanotech 2007, Nanotechnology Conference and Trade Show, Santa Clara, CA, United States, May 20-24, 2007, 2007. **2**: p. 166-169.
48. Sun, Y.-r., et al., *Crystallization and dielectric behavior of polypropylene/carbon nanotubes composites.* Gaofenzi Cailiao Kexue Yu Gongcheng, 2009. **25**(6): p. 67-69,73.
49. Du, F., J.E. Fischer, and K.I. Winey, *Effect of nanotube alignment on percolation conductivity in carbon nanotube/polymer composites.* Phys. Rev. B: Condens. Matter Mater. Phys., 2005. **72**(12): p. 121404/1-121404/4.
50. Kim, D.O., et al., *Transparent flexible conductor of poly(methyl methacrylate) containing highly-dispersed multiwalled carbon nanotube.* Organic Electronics, 2007. **9**: p. 1-13.

51. Berhan, L. and A.M. Sastry, *Modeling percolation in high-aspect-ratio fiber systems. I. Soft-core versus hard-core models.* Phys. Rev. E: Stat., Nonlinear, Soft Matter Phys., 2007. **75**(4-1): p. 041120/1-041120/8.
52. Andrews, R., et al., *Continuous production of aligned carbon nanotubes: a step closer to commercial realization.* Chem. Phys. Lett., 1999. **303**(5,6): p. 467-474.
53. Meier, M.S., et al., *Tearing open nitrogen-doped multiwalled carbon nanotubes.* Journal of Materials Chemistry, 2008. **18**: p. 4143-4145.
54. Ferry, J.D., *Viscoelastic Properties of Polymers*. 3rd ed. 1980, New York: John Wiley and Sons.
55. Williams, G., et al., *Further Considerations of Non Symmetrical Dielectric Relaxation Behaviour arising from a Simple Empirical Decay Function.* Transactions of the Faraday Society, 1971. **67**: p. 1323-1335.
56. Ward, I.M., *Mechanical Properties of Solid Polymers*. 2nd ed. 1983, London: Wiley-Interscience.
57. *DMA Instruction Manual*: TA Instruments Q800 Series.
58. Hedvig, P., *Dielectric Spectroscopy of Polymers*. 1977, New york: John Wiley and Sons.
59. Cole, K.S. and R.H. Cole, Journal of Chemical Physics, 1941. **9**: p. 341-351.
60. Davidson, D.W. and R.H. Cole, Journal of Chemical Physics, 1950(18): p. 1417.
61. Havriliak, S. and S. Negami, *Polymer Symposia.* Journal of Polymer Science 1966. **14**: p. 99-103.
62. McCrum, N.G., B.E. Read, and G. Williams, *Anelastic and Dielectric Effects in Polymeric Solids*. 1967, New York, NY: John Wileys and Sons, Inc.
63. McCrum, N.G., B.E. Read, and G. Williams, *Methacrylate and Related Polymers*, in *Anelastic and Dielectric Effects in Polymeric Solids*. 1991, Dover. p. 238-255.
64. Schonhals, A. and F. Kremer, *Analysis of Dielectric Spectra*, in *Broadband Dielectric Spectroscopy*. 2003, Springer-Verlag: New York, NY. p. 59-98.
65. *Veeco Instruction Manual*: Veeco 7700 Thermal Evaporator.
66. *BDS Instruction Manual*: Novocontrol Concept 40 - Broadband Dielectric Spectrometer.
67. Koeroglu, A., T. Oezdemir, and A. Usanmaz, *Comparative study of the mechanical properties of fiber-reinforced denture base resin.* Journal of Applied Polymer Science, 2009. **113**(2): p. 716-720.
68. Laverty, J.J., et al., *Recycling mixtures of automotive thermoplastics: polycarbonate (PC), poly(methyl methacrylate) (PMMA) and acrylonitrile-butadiene-styrene (ABS).* Polymer Recycling, 1996. **2**(3): p. 159-171.
69. Zemankova, J. and S. Lasek, *Significance and interpretation of morphological features on the brittle-fracture surface of PMMA (Plexiglas).* Strojirenstvi, 1979. **29**(12): p. 736-40.
70. Liu, R.Y.F., et al., *Polymer Interphase Materials by Forced Assembly.* Macromolecules, 2005. **38**: p. 4819-4827.
71. Hirsch, A. and O. Vostrowsky, *Functionalization of Carbon Nanotubes.* Topics in Current Chemistry, 2005. **245**: p. 193-237.
72. Schwarzl, F.R., et al., *Behaviour of unfilled and filled rubbers in shear in the glass-rubber transition region.* Rheologica Acta, 1966. **5**(4): p. 270-275.

73. Logakis, E., et al., *Electrical/Dielectric properties and conduction mechanism in melt processed polyamide/multi-walled carbon nanotube composites.* Polymer, 2009(50): p. 5103-5111.
74. Ash, B.J., R.W. Siegel, and L.S. Schadler, *Glass-transition temperature behavior of alumina/PMMA nanocomposites.* Journal of Polymer Science Part B: Polymer Physics, 2004. **42**: p. 4371-4383
75. Bansal, A., et al., *Controlling the thermomechanical properties of polymer nanocomposites by tailoring the polymer-particle interface.* Journal of Polymer Science Part B: Polymer Physics, 2006. **44**: p. 2944-2950

Table of Nomenclature

Dynamic Mechanical Analysis

δ	Phase lag angle [Radians]
E	Young's modulus [Pa]
E*	Complex modulus [Pa]
E'	Storage modulus, in-phase [Pa]
E''	Loss Modulus, out-of-phase [Pa]
ε	Elastic strain
ε_0	Amplitude of strain
η	Shear viscosity [Pa-s]
σ	Elastic stress [N/m^2]
σ_0	Amplitude of stress [N/m^2]
T_g	Glass transition temperature [^oC]
t	time [s]
ω	Frequency of oscillation [rad/s]

Broadband Dielectric Spectroscopy

A	Area of capacitor plates [m^2]
α	Glass-rubber relaxation
β	Sub-glass relaxation
C	Capacitance [Farads]
C_0	Capacitance of vacuum [Farads]
D	Dielectric displacement [V/m]
D_0	Amplitude of the dielectric displacement [V/m]
D_1	In-phase component of the dielectric displacement [V/m]
D_2	Out-of-phase component of the dielectric displacement [V/m]
d	Distance between capacitor plates [m]

E	Electric field strength [V/m]
E_0	Amplitude of the complex electric field [V/m]
ε_s	Static dielectric constant
ε'	Dielectric constant
ε''	Dielectric loss
P	Polarizability of a material [V/m]
Q	Charge on each of the capacitor plates [Coulomb]
σ	Charge density [Coulumbs/m^2]
V	Potential difference across capacitor plates [Volts]
ω	Frequency of electric field [rad/s]

Vita

Andrew Jonathan Placido was born May 13, 1985 in Lexington, Kentucky. He attended West Jessamine High School and graduated in the top 10 percent of his class, earning the Colonel Scholarship at Centre College to pursue an undergraduate degree in Chemistry. In addition to the Presidential Scholarship, he was also awarded the Les Clem Memorial Scholarship. In the spring of 2007, he graduated with a Bachelor of Science in Chemistry with minors in physics and math.

In the fall of 2007 he joined the University of Kentucky graduate program to pursue a Master of Science degree in chemical engineering under the supervision of Dr. Douglass S. Kalika and Dr. Rodney Andrews. His field of specialization is polymer nanocomposite synthesis and characterization. At present he is working at the Center for Applied Energy Research as an Engineer II and is responsible for the instrumentation and controls for algae reactors to capture CO_2 and the subsequent production of biofuels.